

Metal Electrocatalysts for Hydrogen Production in Water Splitting

Amir Kazemi, Faranak Manteghi,* and Zari Tehrani*

Cite This: *ACS Omega* 2024, 9, 7310–7335

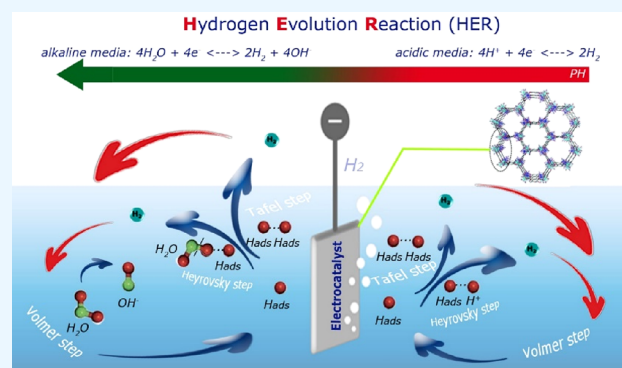
Read Online

ACCESS |

Metrics & More

Article Recommendations

ABSTRACT: The rising demand for fossil fuels and the resulting pollution have raised environmental concerns about energy production. Undoubtedly, hydrogen is the best candidate for producing clean and sustainable energy now and in the future. Water splitting is a promising and efficient process for hydrogen production, where catalysts play a key role in the hydrogen evolution reaction (HER). HER electrocatalysis can be well performed by Pt with a low overpotential close to zero and a Tafel slope of about 30 mV dec⁻¹. However, the main challenge in expanding the hydrogen production process is using efficient and inexpensive catalysts. Due to electrocatalytic activity and electrochemical stability, transition metal compounds are the best options for HER electrocatalysts. This study will focus on analyzing the current situation and recent advances in the design and development of nanostructured electrocatalysts for noble and non-noble metals in HER electrocatalysis. In general, strategies including doping, crystallization control, structural engineering, carbon nanomaterials, and increasing active sites by changing morphology are helpful to improve HER performance. Finally, the challenges and future perspectives in designing functional and stable electrocatalysts for HER in efficient hydrogen production from water-splitting electrolysis will be described.



1. INTRODUCTION

Today, political and economic crises and global concerns such as declining fossil fuel reserves, environmental pollution, acid rain, global warming, overcrowding, rising consumption, and economic growth are challenging scientists to find appropriate solutions to the world's energy problems.^{1,2} This problem can only be rectified by replacing green and renewable energy sources.³ In recent decades, hydrogen has been called the best and most promising alternative due to its high gravitational energy density, environmental friendliness, and combustion without producing pollutants.⁴ Meanwhile, the energy density of hydrogen is approximately equivalent to 33.5 kWh/kg of usable energy, while this amount of energy for diesel is about 13 kWh/kg.⁵ In other words, the energy of 1 kg of hydrogen, which is used to power the electric motor in fuel cells, is equivalent to a gallon of diesel. In another comparison, diesel has a little lower energy density (45.5 MJ/kg) than gasoline (45.8 MJ/kg). On the other hand, hydrogen has an energy density of approximately 120 MJ/kg, almost three times more than diesel or gasoline.⁶ In the past decade, with the advent of electric propulsion, it has become clear that these propulsions are much more efficient than internal combustion engines, making energy change even more important. In internal combustion engines, almost half of the energy is used to produce heat, while electric vehicle (EV) engines waste less than 10% of energy as heat.⁷ Another appealing feature of hydrogen is price. The diesel price is

currently around \$3.00 per gallon, and with the recent decline in Iran's oil production, it is reasonable to expect a further increase in the price of diesel.⁸

Green hydrogen, also known as renewable hydrogen, is hydrogen that is manufactured using only renewable energy, typically by the process of water electrolysis (WE).⁹ The hydrogen evolution reaction (HER) through water splitting has many advantages, including that the reaction can be performed at room temperature and atmospheric pressure. Selective production of oxygen and hydrogen is possible in this process, thus eliminating the gas separation step.^{10,11} Also, the source used (H₂O) and the products made (O₂ and H₂) are environmentally friendly. It is worth noting that despite the tremendous advantages, the HER has limitations due to its high electric power consumption and the use of optimized catalysts.¹² However, renewable energy application systems, including the HER, depend highly on the appropriate electrocatalyst type.^{11,13} State-of-the-art precious metals and their compounds are active materials for HER and oxygen evolution reactions (Pt for HER,

Received: October 10, 2023

Revised: December 28, 2023

Accepted: December 29, 2023

Published: January 29, 2024



IrO₂ and RuO₂ for OER, etc.).¹⁴ Up to now, Pt is the most efficient catalyst for HER, which requires very small overpotentials even at high reaction rates.¹⁵ Despite the high efficiency of noble metals, high cost, and scarcity of reserves being barriers to large-scale application, this requires using more affordable and abundant materials for the electrocatalyst.^{16,17}

The purpose of this study is to address the pressing environmental concerns regarding energy production through the efficient and sustainable production of hydrogen through water splitting. Hydrogen is a promising source of clean energy, and catalysts play a crucial role in the HER during water splitting. Platinum (Pt) exhibits excellent electrocatalytic activity for HER, but its widespread adoption is hampered by cost considerations. We overcome this challenge by turning to transition metal compounds, which offer both electrocatalytic activity and electrochemical stability. An analysis of the current state and recent advancements in nanostructured electrocatalysts for both noble and non-noble metals will be presented in this investigation. To enhance HER performance by increasing active sites through morphological modifications, we will explore various strategies, such as doping, crystallization control, structural engineering, anion doping in addition to cation doping, and the use of carbon nanomaterials. The final section of the presentation will discuss the challenges that lie ahead and offer future perspectives on how to design functional and stable electrocatalysts for the HER in order to enable efficient hydrogen production by water-splitting electrolysis.

2. HER

Currently, hydrogen is mainly used as a raw material in the chemical industry, and its use as a fuel for energy supply has not yet become large-scale. The most economical and common hydrogen generation methods are steam methane reforming (SMR), coal gasification (CG), and WE¹⁸ as shown in Table 1.

Table 1. Three Main Criteria for Hydrogen Production on an Industrial Scale

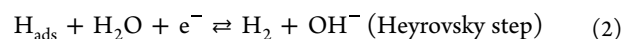
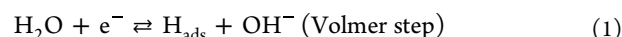
criteria	source	production	reaction
steam methane reforming	methane, steam	H ₂ , CO ₂	CH ₄ + 2H ₂ → 4H ₂ + CO ₂
coal gasification	coal, steam	H ₂ , CO ₂	C + 2H ₂ O → 4H ₂ + CO ₂
water electrolysis	water	H ₂ , O ₂	2H ₂ O → 2H ₂ + O ₂

The SMR and CG have a price advantage, but they consume fossil fuels and are environmentally damaging. One of the above methods, the WE process, is a green energy method, which produces ultrapure hydrogen (>>99.999) but costs more than conventional methods.¹⁹ IEA (International Energy Agency) analysis shows that renewable energy's cost of hydrogen production could fall 30% by 2030.²⁰ Although WE can solve environmental problems as a renewable energy production technology, the application of this method is still minimal.²¹ Nevertheless, adequate studies and research are underway to improve this technology to reduce production costs on an industrial scale. In the electrolysis of water, the hydrogen–oxygen bond in a water molecule is broken by electrical power.²²

The ability to carry out WE without the utilization of precious metal catalysts in the HER and OER makes it a desirable option in justifying the economics of hydrogen production.²³ Therefore, developing electrocatalysts with high activity and long-lasting stability to improve the kinetic energy of electrolyte decomposition is critical for potential implementation and

useful applications. Electrochemical WE is a promising technology to generate hydrogen fuel from water renewably; this is the process of converting water to pure and stable hydrogen that is made up of two half-cell reactions: the oxygen evolution (OER) and the hydrogen evolution (HER) reaction processes.²⁴ Due to the high power consumption in this process, catalysts can reduce the required potential by their performance. Precious metal electrocatalysts (especially Pt-based) show the best performance for the molecular dissociation of water in highly acidic electrolytes, although their HER activities are significantly reduced under alkaline conditions.²⁵ As a result, considerable effort has gone into developing effective and sustainable electrocatalysts to replace precious metal catalysts. Chemically, bond-breaking and forming new bonds are effective ways to convert and store energy. According to this principle, WE, also called water splitting, is the process of using electricity to break down water molecules and form their constituent elements.²⁶ The process of water splitting without using scarce and expensive electrocatalysts to produce hydrogen has made it an attractive option to make renewable energy more economical in recent years.

2.1. Fundamentals of the HER. Water, unlike fossil fuels, is an abundant and renewable resource on Earth, so the hydrogen (H₂) produced by water splitting can be called the best solution to provide a carrier of green and renewable energy. The HER is a multistep process involving adsorption, reduction, and desorption that takes place on the electrode surface and produces gaseous hydrogen. The three general mechanisms in the HER involve the following reaction steps:



The HER mechanism begins with the Volmer step, which is the dissociation of a water molecule and the absorption of H⁺ at the electrode surface (electrocatalysis). The process is then followed by the chemical reaction of the Heyrovsky step or the Tafel step. As per the intrinsic nature of electrocatalysis, the reaction can be carried out with the reaction of two adsorbed H (reaction) or the H adsorption with H⁺ (Heyrovsky reaction) from the electrolyte to release the H₂ molecule. Whatever the reaction steps, due to the adsorption of H in the reaction, facilitating the adsorption process is the main task of the electrocatalyst.²⁷ The free energy from absorption of H in Pt is near to the thermoneutral state ($\Delta G_{\text{H}^*} \approx 0$). That is why Pt is widely recognized as the greatest HER electrocatalyst available to date. Numerous articles have reported that the Tafel step in the high potential of the HER mechanism is insignificant, and the Volmer–Heyrovsky mechanism is used to carry out the reaction.^{13,28}

2.2. Acidic and Alkaline Media. The key half-reaction for hydrogen production in water splitting occurs at the cathode, which involves the transfer of two highly dependent electrons in environmental conditions. The alkaline environment is now the focus of hydrogen development through the HER to substitute clean fuel for different energy systems. Due to an extra water dissociation process, the kinetics of this reaction are sluggish and cause a significant reduction in electrocatalytic performance. Therefore, modern electrocatalysts can perform well in acidic environments.²⁹ The electrocatalyst's effectiveness in an alkaline environment is controlled by theoretical studies based on two

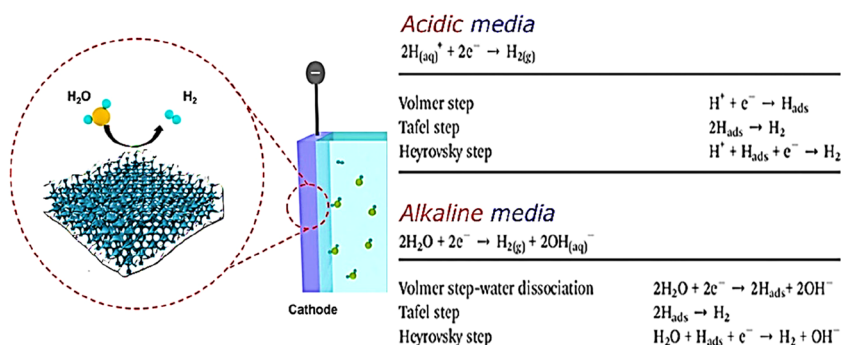


Figure 1. Different mechanisms on the surface of the catalyst in acidic and alkaline environments.

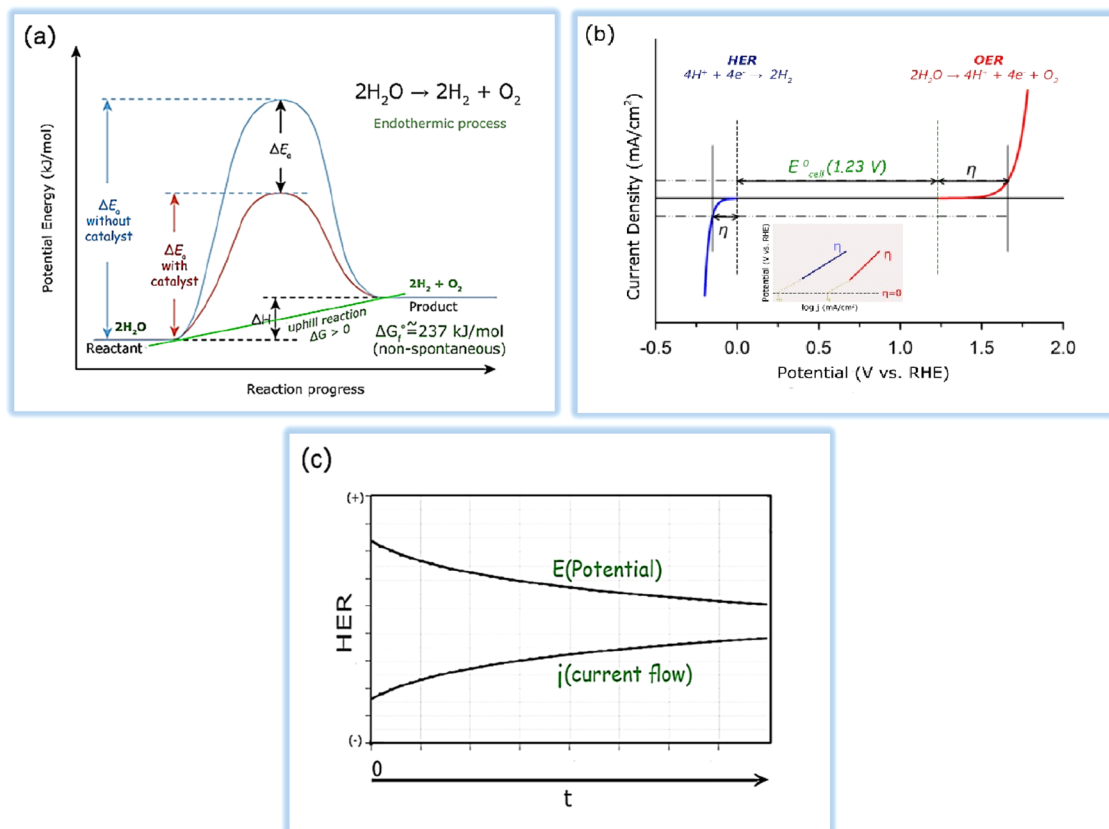


Figure 2. Schematic illustration of the (a) role of the catalyst in reducing the activation energy barrier in the reaction; (b) performance evaluation items of the electrocatalyst, including activity in terms of overpotential, Tafel slope, and exchange current density; (c) performance evaluation items of the electrocatalyst, including stability in terms of current and potential/time curves.

factors: water dissociation and then hydrogen-bonding energy. Each electrode with a higher ability to dissociate the water molecule and a better capability to bond to produce a hydrogen atom can therefore be a better electrocatalyst for the HER process in an alkaline environment.³⁰ As shown in Figure 1, an electrocatalytic reaction occurring in acidic and alkaline environments follows different mechanisms. In an acidic environment, the mechanism is performed by combining the electrolyte's proton and one electron from the electrode surface, which is expressed as the Volmer path. The next path is the Tafel path, which is formed by the combination of hydrogen atoms with neighboring atoms. The Heyrovsky path is the latter path, which consists of combining one electron from the electrode surface and another proton from the solution (electrolyte). In alkaline environments, protons are no longer present in electrolytes. Thus, the mechanism begins with dissociating a

water molecule, called the Volmer pathway. Then, the Tafel or Heyrovsky path continues to produce hydrogen.³¹

Three fundamental phases, one chemical and two electrochemical, make up the electrocatalytic evolution of H_2 on the electrode surface in an alkaline solution. The first stage is the electrochemical separation of water to generate a hydrogen molecule, which is adsorbed on the surface of the electrode via the Volmer reaction. The next step is an electrochemical process for the hydrogen adsorbed to form H_2 , known as the Heyrovsky reaction, or chemical reaction, known as the Tafel reaction.

It should be noted that the Tafel slope values illustrate the HER process mechanism by describing the potential difference necessary to raise or reduce the current density by 10×. How the current is produced in response to the change of potential applied to the electrode is represented by the Tafel slope. Accordingly, less overpotential is required to obtain high current

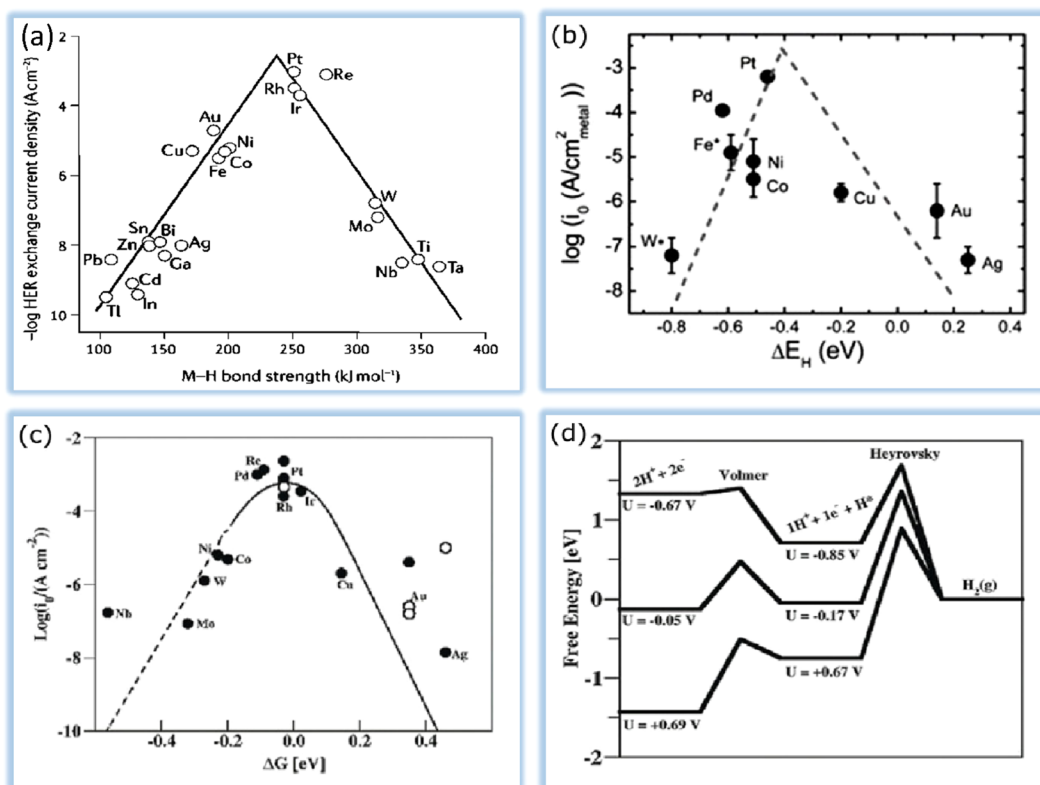


Figure 3. (a) Volcano-type dependence between the exchange current density and metal–hydrogen (M–H) bond strength. Data taken from ref 41. (b) Exchange current densities, $\log(i_0)$, on monometallic surfaces plotted as a function of the calculated HBE. The i_0 s for non-Pt metals were obtained by extrapolation of the Tafel plots between -1 and -5 mA cm^{-2} disk to the reversible potential of the HER and then normalization by the ESAs of these metal surfaces. Data taken from ref 38. (c) A volcano plot containing measured j_0 plotted versus the computed ΔG_H at equilibrium potential in acidic conditions. Data taken from ref 39. (d) Standard free energy diagram for the Volmer–Heyrovsky route HER under different potentials. Data taken from ref 39.

at a lower Tafel slope (mV/decade). In general, due to the high overpotential of hydrogen, significant electrical energy is required to perform the whole process. Therefore, reducing the cathodic overpotential is one of the challenges in making this process economical. The best way to minimize the cathodic overpotential is to use optimized electrocatalysts such as Pt at the cathode to perform the HER. An acidic medium has less overpotential than an alkaline environment. However, the high cost of membranes and stable electrocatalysts in an acid corrosive environment is one of the disadvantages of this medium.^{16,32}

2.3. Rate of Reaction. A thermodynamic potential of 1.23 V at 25 °C has been calculated for the electrochemical water-splitting reaction (1 atm). In this reaction, which is an uphill reaction, a large kinetic barrier must be overcome in addition to being expressed by a positive value of G (Gibbs free energy). Figure 2a demonstrates that catalysts are essential in reducing the kinetic barrier. This reaction necessitates a greater potential than the thermodynamic potential to overcome the kinetic obstacle (1.23 V). The performance of a catalyst is evaluated based on critical parameters such as activity, stability, and efficiency. The Tafel slope and overpotential can show the activity of the catalysts and the density of the exchange current derived from polarization curves (Figure 2b). Overpotential is a fundamental description for evaluating the activity of electrocatalysts. Overpotential changes and current flow over time are indicators of stability (Figure 2c). The efficiency of an electrocatalyst can be evaluated by comparing experimental

results against theoretical predictions with faradaic efficiency and turnover frequency.³³

The total reaction rate is determined by the free energy of hydrogen adsorption (ΔG_H). If the hydrogen molecule attaches poorly to the surface of the catalyst, the Volmer step (adsorption) will slow down the total reaction rate. However, if the bond between the catalyst surface and the hydrogen is stronger than usual, the desorption is slow, meaning that the Heyrovsky/Tafel phase limits the velocity. Therefore, $\Delta G_H^* \approx 0$ is a required (but inadequate) prerequisite for an active HER catalyst. With these explanations, it can be concluded that one of the characteristics of an effective catalyst is that the middle bond of the reaction is neither too strong nor too weak.^{34,35}

2.4. Pseudocapacitance. In the HER process, hydrogen must be adsorbed on the surface of the electrocatalyst in the first step. In the next step, the adsorbed hydrogen must be separated from the electrocatalyst surface and returned irreversibly to the electrolyte. This electrocatalyst pseudocapacitive characteristic is critical to HER performance. In hydrogen adsorption, practically all HER electrocatalysts are excellent pseudocapacitors. In order to desorb all of the hydrogen absorbed, a good pseudocapacitor must be highly efficient. Therefore, studying pseudocapacitive performance before the HER potential offers vital information on electrocatalyst efficiency. The optimal pseudocapacitive performance, which is typified by a rectangular shape in cyclic voltammetry (CV), is significantly more closely related to HER electrocatalytic activity.³⁶

2.5. Volcano Plots. As stated in the previous sections, theoretical simulations prove that HER activity is closely

connected to hydrogen adsorption (H_{ads}) and that the free energy of hydrogen adsorption (ΔG_{H}) can accurately characterize hydrogen evolution. Also, the moderate amount of hydrogen-bonding energy in the HER process is of great advantage. The volcano curve, as illustrated in Figures 3a and 3b, can compare the behaviors of various metals in acidic and alkaline environments.^{37,38} Pt is the superior electrocatalyst for HER in both mediums, as demonstrated in the plots, because it has the appropriate hydrogen adsorption energy and hence provides the largest exchange current density. An acidic medium has less overpotential than an alkaline environment. Nevertheless, it is less used due to the corrosion of electrocatalysts. Also, the alkaline environment is critical due to non-noble electrocatalysts. Alkaline water splitting is an excellent way to produce pure hydrogen with high purity. This technology is environmentally friendly and does not emit any carbon dioxide. Pt and Pt-based alloys perform very well in the HER due to their low activation overpotential. As mentioned, HER activity is very often lower in alkaline media than in acidic conditions. This is primarily due to the slowing down of the water dissociation phase. However, alkaline electrolysis is preferred on an industrial scale. It is critical to consider the bonding of hydrogen species and the water dissociation potential when designing electrocatalysts with high alkaline HER performance. According to Figure 3c and Figure 3d,³⁹ both the thermodynamic influence of ΔG_{H} and the hydrolysis kinetics affect the progress of the reaction. The volcanic plot predicts that metals such as PGMs are on top of the volcano plot with the ideal H binding energy and show the highest activity. Similar to the acidic media, a volcano plot can describe the relationship between H bonding energy values and HER exchange current density at alkaline pH. This description can be defended by experimental studies and density-functional theory (DFT).⁴⁰

2.6. Kinetic Isotope Effect (KIE). An important method for studying chemical reactions is the kinetic isotope effect (KIE). This theory is based on the observation that the rate of a reaction can vary with atom mass. A particle's mass affects the energy of its vibrational and rotational states, which, in turn, affects the probability of tunneling. Tunneling is a quantum mechanical process that allows particles to pass through potential barriers without having enough energy to overcome them.

Primary and secondary KIEs are the two main types. There is a primary KIE when the difference in mass only exists between the atoms involved in the rate-determining step between two isotopically substituted reactants. A secondary KIE is the ratio of the rates of reaction between two isotopically substituted reactants, where the mass difference is not between the atoms. A KIE can be used to identify the rate-determining step in a reaction. If a primary KIE is observed, then the rate-determining step must involve breaking or forming a bond between the isotopically substituted atoms. Conversely, if a secondary KIE is observed, the rate-determining step must not involve breaking or forming a bond between the isotopically substituted atoms. By providing information about the transition state's energy, KIEs can also be used to study the mechanism of a reaction. In the case of a primary KIE, the transition state energy for the lighter isotope must be lower than for the heavier isotope. In contrast, if a secondary KIE is observed, then both isotopes must have the same energy of the transition state. Aside from primary and secondary KIEs, equilibrium isotope effects and kinetic secondary isotope effects are also types of KIEs. In equilibrium isotope effects, the equilibrium constants of two isotopically substituted reactions are compared. Kinetic secondary isotope

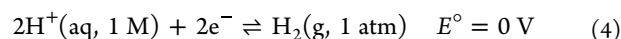
effects are calculated using the ratio of the rate constants of two isotopically substituted reactions in which the difference in mass is not between atoms involved in the rate-determining step but between atoms involved in the equilibrium constant. Chemical reactions can be studied using a KIE. It is possible to use them to identify the rate-determining step, to determine the energy of the transition state, and to study the mechanism of reactions that are difficult to study using other methods. An electron is transferred from the electrode to a hydrogen ion in the electrolyte as part of the HER process. As an electrolyte, both H_2O and D_2O have been used to study the KIE of the HER. When D_2O is used instead of H_2O in these studies, the rate of the reaction is approximately 6 times faster. Since the D^+ ion is heavier than the H^+ ion, it moves through the electrolyte more slowly. Based on the KIE for the HER, the following mechanism can be proposed:

- (1) An electron is transferred from the electrode to a hydrogen ion in the electrolyte, forming a hydronium ion.
- (2) The hydronium ion dissociates into a proton and water molecule.
- (3) The proton tunnels through the water molecule and attacks the surface of the electrode, forming a hydrogen atom.
- (4) The hydrogen atom desorbs from the surface of the electrode, forming hydrogen gas.

A KIE indicates that an electron is transferred from the electrode to a hydrogen ion in the electrolyte to determine the rate of the reaction. The isotope effect is much larger for this step than for any of the other steps.⁴²

3. HER ELECTROCATALYSTS REQUIREMENTS

The disparity between the electrical potentials of each electrode determines the potential of an electrochemical cell. It is impossible to determine the electrical potential of a single electrode; for this purpose, we can set an electrode to zero and use it as a reference. This selected electrode is called the standard hydrogen electrode (SHE). This electrode is a reference for measuring the activity potential of different materials relative to each other. The reduction half-reaction selected for reference is



In the above relationship, E° stands for the standard reduction potential (at a standard temperature of 25 °C and pressure, 1 atm, 1 M for solution), and at all temperatures the voltage is defined as zero (0 V vs RHE). According to theoretical calculations, the potential of the cell along the entire water-splitting path is 1.23 V.⁴³ This reduces efficiency and kinetics. Designing and utilizing highly efficient catalysts to reduce the overpotential for OER and HER to produce H_2 and O_2 is one efficient way to do this. It is crucial to comprehend the criteria used to assess and contrast the electrocatalytic activity of particular materials and to establish test procedures. Unfortunately, no coordinated effort has been made to develop an integrated test protocol or a way to present quantitative electrocatalytic data. In studies, the performance of electrocatalysts is usually evaluated with the following parameters.⁴⁴

3.1. Overpotential, Tafel Slope, and Exchange Current Density. The overpotential (η) component is a fundamental descriptor for assessing the electrocatalysts' behavior, which is the difference between the theoretical half-reaction reduction potential and the actual cell potential. Suitable electrocatalysts for HER should have a small overpotential because the amount

of low overpotential is directly related to the high electrocatalytic activity. Water splitting occurs at a cell potential of 1.23 V (0 V for HER and 1.23 V for the OER). Both HER and OER processes need additional potential, mainly from the intrinsic activation obstacles present. The applied potential must be increased for the reaction to occur.^{45,46} Usually, the overpotential value corresponds to the current density such as 10 mA cm⁻² ($\eta = 10$) and/or 100 mA cm⁻² ($\eta = 100$).

Another approach for measuring HER electrocatalyst activity is to calculate Tafel parameters, the values of which are typically determined by examining the polarization curve as a logarithmic current density diagram ($\log(j)$) vs iR -compensated overpotential (η). The Tafel slope represents the kinetic relationship between the overpotential and the current density in the electrocatalyst, which is expressed by eq 5:

$$\eta = a + b \cdot \log|j|, \text{ where} \quad (5)$$

$$a = \frac{2.303 \cdot RT}{\alpha F} \log(j_0) \quad (6)$$

$$b = \frac{-2.303 \cdot RT}{\alpha F} \quad (7)$$

In this equation, η is the overpotential, and j is the current density.

The Tafel slope (b) and the exchange current density j_0 are determined by obtaining the current at a potential of zero. As stated, the overpotential is the difference among the electrodes' potential under the equilibrium potential (E_e) and current load (E_j). According to eq 5, the Tafel slope (b) is an intensive quantity independent of the surface area of the catalyst, and its value is defined by the rate-determining stage and its location in the reaction process. In contrast, j_0 is a large quantity and depends on the surface area of the catalyst and indicates easy electron transfer with small activation energy. An active electrocatalyst should have a low Tafel slope and a large j_0 . A lower Tafel slope suggests a large increase in current density as a function of overpotential variation (i.e., the kinetics of the electrocatalytic reaction are faster).^{47,48}

The exchange current density (j_0) can be defined as the readiness of the electrode to continue the electrochemical reaction, so the higher the exchange current density, the more active the electrode surface. It describes the intrinsic charge transfer exchange current density under an equilibrium state. Increased exchange current densities indicate higher charge transfer rates and better reaction progress.⁴⁹ Therefore, it can be concluded that for a better electrocatalyst, a higher exchange current density and a lower Tafel slope are expected. The scan rate used to obtain the potentiodynamic polarization curve should not be overlooked because this parameter strongly affects the values obtained for the current density and Tafel slope. Potentiostatic method curves or recorded polarization curves should thus be assessed at the slowest scan rate available. The exchange current density (j_0) indicates the intrinsic interactions and charge transfer activity between the electrocatalyst and the reactant. High exchange current density usually reflects the excellent performance of the HER reaction electrocatalyst. However, it should be noted that obtaining direct exchange current density is challenging, and we can only get the total current density from the Tafel equation experiments.⁵⁰

3.2. Electrochemically Active Surface Area (ECSA). The electrode material's electrochemical surface area (ECSA) is one of the fundamental phenomena in selecting electrocatalysts,

indicating the area of the electrode material available to the electrolyte. It has been proven that it is challenging to measure the electrochemically active surface of any material as an electrode. This surface is used for charge transfer and/or storage in electrochemical cells (galvanic/electrolytic). The electrode surface may be expanded using a variety of techniques. These include using nanostructures, cyclic voltammetry (CV), and linear sweep voltammetry (LSV).⁵¹

3.3. Faradaic Efficiency. Faraday efficiency (also known as current efficiency) is another parameter used to assess the activity of the HER electrocatalyst. In place of the side reaction, faradaic efficiency (FE) calculates the amount of charges (electrons) in the desired reaction. In the HER process, FE is the ratio of experimentally identified H₂ compared to the theoretical quantity H₂. This ratio of experimental H₂ to theoretical H₂ is calculated using a current density based on 100% faradaic output. The faradaic efficiency is calculated under two parameters: the total amount of hydrogen produced nH_2 (mol) and the total amount of charge Q (C) transferred from the cell using eq 7. The total charge is determined by integrating the current, and the total amount of hydrogen generated is determined by using gas chromatography (GC) or the water displacement method.⁵²

$$\text{Faradaic efficiency} = nH_2 / (Q/2F) \quad (8)$$

F is the Faraday constant, $\cong 96\,500$ C/mol.

3.4. Turnover Frequency. The turnover frequency (TOF) of a catalytic center quantifies its particular activity by the number of reactants transformed to the chosen product per unit time. The amount of TOF for HER and OER is calculated based on the following equations:

$$\text{TOF HER} = JA/2nF \quad (9)$$

$$\text{TOF OER} = JA/4nF \quad (10)$$

where A represents the area of the working electrode and J is the current density; the number 2 represents the electrons for H₂/mol, and the number 4 represents the electrons for O₂/mol; also, n embodies the mole number of active sites, and F is the Faraday constant.

In experiments, measuring TOF is not easy for most solid-state catalysts. In this case, the catalyst's surface atoms are not catalytically active or uniformly available. A presence of HER bubbles on the electrode surface causes an excessive rise in potential and disturbs the active surface. Admittedly, TOF values cannot provide much accuracy, but they can still assist in linking catalyst activity.⁵³

3.5. Hydrogen-Bonding Energy. In the hydrogen evolution reaction (HER), an electrochemical process that generates hydrogen gas from water splitting, hydrogen-bonding energy (HBE) plays a crucial role. Hydrogen bond energy describes the strength of hydrogen atoms' interaction with neighboring atoms, usually oxygen atoms in water or on the catalyst surface. The interaction affects the overall kinetics of the HER, affecting the rate of hydrogen evolution and the stability of adsorbed hydrogen species. Adsorption of hydrogen intermediates on the catalyst surface is made easier by a strong hydrogen bond between hydrogen atoms and the catalyst surface. If the HBE is too strong, it can prevent hydrogen molecules from desorbing, reducing hydrogen evolution efficiency. In order to achieve efficient and sustainable HER, an optimal HBE must be in place. Numerous techniques have been used to study the effects of HBE on HER activity, including

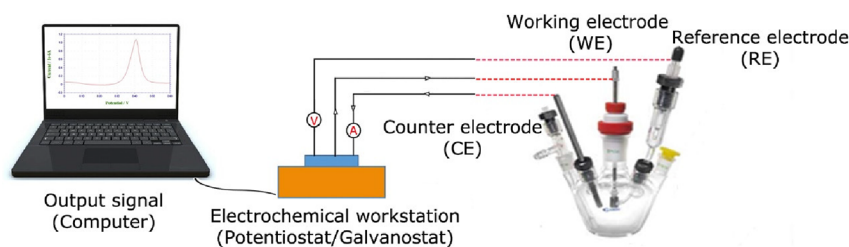


Figure 4. Three-electrode system with working electrodes, counters, and reference electrodes.

theoretical calculations, spectroscopic studies, and electrochemical measurements. Catalysts with a moderate HBE typically exhibit higher HER activity than those with a too weak or too strong HBE, according to these studies. A moderate HBE allows for efficient electron transfer and hydrogen desorption without hindering hydrogen intermediate formation. HER activity is also affected by the distribution of HBE sites on the catalyst surface in addition to the strength of the HBE. The uniform distribution of HBE sites promotes the formation of stable intermediates and efficient hydrogen evolution by providing hydrogen atoms with suitable binding sites. In order to develop efficient HER catalysts, it is essential to optimize HBE. Researchers can design catalysts with the desired HBE properties to achieve high HER rates and stability by understanding the relationship between HBE and HER activity. The development of sustainable hydrogen production technologies depends on this. In order to achieve efficient HER, an optimal HBE is necessary. Catalysts with a moderate HBE typically exhibit higher HER activity than those with either a weak or a strong HBE. A moderate HBE promotes the overall HER process by stabilizing adsorbed hydrogen species and facilitating their desorption.

Relationship between HBE and HER Activity. A complex relationship exists between the strength of the HBE and the activity of the HER. Strong HBEs can indeed stabilize adsorbed hydrogen species, but they can also hinder hydrogen desorption if they are too strong. Due to the strong HBE, hydrogen molecules cannot break away from the catalyst surface. Thus, the catalyst becomes saturated with hydrogen atoms, and the overall HER rate decreases.

Factors Affecting HBE. There are several factors that can affect the HBE between hydrogen atoms and the catalyst surface, such as the following:

- (1) Nature of the catalyst surface: HBE can be significantly affected by the type of metal or material used for the catalyst surface. Catalysts containing a high density of oxygen-containing groups, such as hydroxides and oxides, tend to exhibit stronger HBE than catalysts containing a lower density.
- (2) Preparation methods: A catalyst's preparation method can also affect its HBE. The formation of HBE is more likely to occur in catalysts prepared using methods that introduce defects or roughness into their surfaces.
- (3) Electrolyte composition: HBE can also be affected by the electrolyte composition. Electrolytes with higher pH values, for example, tend to form stronger HBE than electrolytes with lower pH values.

Optimizing HBE and Impact on Sustainable Hydrogen Production. Developing efficient HER catalysts requires optimizing HBE. Scientists can design catalysts with high HER rates and stability by understanding the factors that influence

HBE and tailoring the catalyst surface and preparation methods accordingly. Hydrogen production technologies require efficient HER catalysts for advancement. Optimizing HBE can enhance the performance of HER catalysts, making them more suitable for practical hydrogen production applications, such as fuel cells and hydrogen storage. The hydrogen bonding energy (HBE) determines the stability of adsorbed hydrogen species, the desorption of hydrogen molecules, and the overall efficiency of hydrogen evolution reactions (HER). To develop efficient HER catalysts and realize the potential of sustainable hydrogen production technologies, it is crucial to understand and optimize HBE.

3.6. Stability. Another important parameter for choosing the suitable HER electrocatalyst is stability. There are two approaches to assess the stability factor. One is LSV or CV; the other is potentiostatic or galvanostatic electrolysis by long-term chronopotentiometric (CP) or chronoamperometric (CA) tests. This voltammetric method is utilized to compare the overpotential modifications, before and after a certain period of cycles for 1 000–10 000 cyclic voltammograms at a scan rate such as 5–50 mV s⁻¹.

In a CV cycle, the higher the number of cycles, the higher the accuracy, and the better it can be to reach a few thousand cycles by a high potential limit of up to 0 V vs RHE. Changes in the parameters of the polarization curve as well as overpotential (at a specific current density) are evaluated before and after the CV cycle to measure stability.^{54,55} The lesser the rate of change, the greater the material's stability. It is widely acknowledged that assessing a catalyst's long-term stability is sufficient for around 12 h. However, it is strongly advised that the measures be evaluated for at least 240 h in order for the stability results to be at least somewhat industrially defensible. An HER electrocatalyst must be usable for several thousand hours to be ready for use on a large scale. Accelerated experiments usually last only a few hours at best. Such expedited testing may not give exact operational information for industrial-scale assessment. However, this time is clearly restricted from an industrial viewpoint, and further testing is required before larger-scale implementation.^{56,57}

3.7. Electrochemical Methods (Three-Electrode Cell). In the HER process, a rotating disk work electrode (RDE) is suggested to obtain accurate experimental data. With high accuracy, this electrode can quantify the mass transfer rate and reaction kinetics well. The RDE is a working electrode used in three-electrode systems for voltammetry of electrochemical studies when examining the reaction mechanisms of redox chemistry, among other chemical phenomena.⁵⁸ The electrode is connected to an electric motor with excellent control over the rotation speed of the electrode. The electrode rotates during the test and induces a flux of analyte to the electrode depending on the applied voltage. The structure of this electrode consists of a conductive disk made of a noble metal or glassy carbon

surrounded by a nonconductive material such as a polymer or an inert resin. According to Figure 4, in an electrochemical system, the working electrode (WE) is often used in conjunction with a counter electrode (CE) and a reference electrode (RE) in a three-electrode system.^{54,59}

3.8. Measurement Pitfalls and Data Interpretation in HER Studies. Electrochemical measurements play a crucial role in studying the HER and evaluating the performance of catalysts. However, there are several challenges and pitfalls that researchers may encounter during these measurements, which can affect the accuracy and reliability of the obtained data. In this section, we summarize some common pitfalls and provide guidance for addressing them.

Electrode Fouling and Surface Contamination. One of the major challenges in HER measurements is electrode fouling and surface contamination. Over time, the electrode surface can become covered with reaction intermediates or byproducts, leading to altered electrochemical behavior and inaccurate measurements. To mitigate this issue, careful electrode preparation, regular cleaning, and appropriate experimental conditions should be employed. Techniques such as cyclic voltammetry and electrochemical surface cleaning can help remove adsorbed species and restore the electrode surface.

Electrolyte Effects. The choice of electrolyte can significantly influence HER measurements. Different electrolytes can have varying pH, ionic strength, and composition, resulting in different reaction kinetics and performance of catalysts. It is crucial to carefully select an electrolyte that is suitable for the specific HER system under investigation. Additionally, understanding the effects of electrolyte composition on the reaction mechanism and kinetics is essential for accurate data interpretation.

Proper Data Analysis Techniques. Interpreting electrochemical data accurately is crucial for understanding the performance of HER catalysts. Common pitfalls in data analysis include incorrect baseline subtraction, improper fitting models, and overlooking potential artifacts. Researchers should carefully select appropriate analysis techniques, such as Tafel analysis or electrochemical impedance spectroscopy, and ensure proper data processing and fitting procedures. It is also important to consider potential artifacts, such as capacitive currents or double-layer charging effects, and account for them in the data analysis.

By being aware of these pitfalls and employing appropriate measures, researchers can improve the accuracy and reliability of their electrochemical measurements and data interpretation. Addressing these challenges is essential for advancing our understanding of HER catalysts and developing efficient hydrogen production technologies. Overall, by summarizing the common pitfalls and providing practical guidance for measurement and data interpretation, researchers can navigate through the challenges inherent in HER studies and obtain more accurate and reliable results.

4. HER ELECTROCATALYSTS

Given the materials investigated as candidate electrocatalysts for HER in the water-splitting process, a coherent method for presentation and comparison is critical.^{56,58} The approach employed in this study is to categorize materials into three major groups:

- (1) Noble metals with compounds and alloys

- (2) Low-cost transition metal-based materials without precious metals
- (3) MOF-derived material-based electrocatalysts

Today, efforts are focused on developing low-cost metal-based electrocatalysts with high stability and performance and are considered an essential and promising candidate for the industrial scale.

4.1. Noble Metal-Based Electrocatalysts. The electrocatalytic performance of noble metals, such as Pt group metals (PGMs, including Pt, Pd, Rh, Ru, and Ir), is appealing for HER.⁶⁰ The Volcano diagram shows that these materials are at the top of the curve. However, due to their scarcity and high price, the commercial application of these noble metal electrocatalysts is constrained.⁶¹ Rational design of catalysts with minimal noble metal load and high usage of other metals is crucial to overcoming this difficulty.⁶² The trend of Pt activity is (111) < (100) < (110) according to the single-crystal aspects with a low Pt index in the HER process. The justification for this trend can be attributed to the presence of H_{opd} (overpotential deposition, weakly adsorbed state) reaction, which is most prevalent at level (110). Therefore, the activity of the Pt surface (110) in the role of electrocatalyst can be greater than that of the other two surfaces.⁶³ Therefore, modification and optimization of geometric parameters of noble metal-based electrocatalysts while maintaining activity have been investigated.⁶⁴ The activity of Pt electrocatalysts in an alkaline environment is typically lower than in an acidic environment as a benchmark. This is because the dissociation of water at the Pt surface is inefficient, leading to this electrocatalyst's weak activity in the electrolyte. Pt coupling with water dissociation promoters is a popular technique for improving the electrocatalytic capabilities of HER in an alkaline environment to compensate for this.⁶⁵ The optimization of geometric parameters and efficient modifications in structure while preserving electrocatalytic activity have been thoroughly explored as a result of the right deployment of Pt-based electrocatalysts. Loading Pt nanoparticles on high-surface carbon is a simple and cost-effective technique to generate active HER electrocatalysts for this purpose. The most common method is carbon black with 20% by weight of platinum put on it (Pt/C), which may generate one of the lowest overpotentials (46 mV at 10 mA cm⁻²) in alkaline circumstances. Pt/C catalysts are frequently utilized as a standard for catalysts created for the HER reaction because of their superior outcomes and performance. Due to its lower cost and similar electronic structures, Ru is always considered a potential candidate to replace Pt for water electrolysis. However, dissolution and stability problems must be thought out.^{45,66}

The element titanium is also widely used in electrocatalytic reactions. Titanium dioxide (TiO₂) is a transition metal oxide that has been extensively studied for its potential application in the hydrogen evolution reaction (HER). However, the traditional crystalline TiO₂ is generally considered as an inactive material for HER with disappointing performance. This is due to its poor electrical conductivity and unfavorable hydrogen intermediates (H_{ads}) adsorption/desorption capability. In order to activate TiO₂ for HER, theoretical calculations and experimental studies have been carried out to investigate the effect of structural and electronic properties on the hydrogen adsorption free energy (ΔG_{H^*}). The results suggest that the hydrogen adsorption free energy could be optimized through tuning the structural and electronic properties of TiO₂. For example, amorphous TiO₂ with disordered atom arrangement

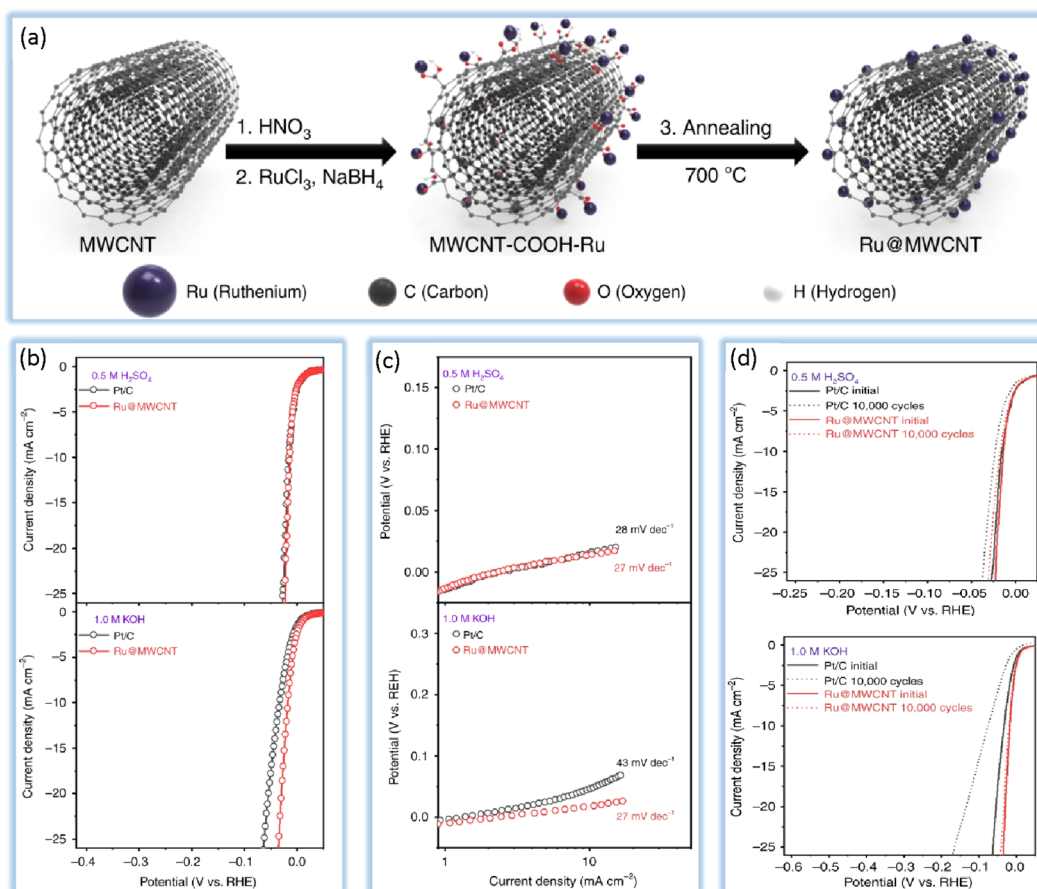


Figure 5. (a) Schematic illustration of the process steps for forming Ru@MWCNT catalyst; (b, c) electrochemical HER performance of the Ru@MWCNT and Pt/C catalysts; polarization curves and corresponding Tafel plots in N₂-saturated 0.5 M aq. H₂SO₄ solution and 1.0 M aq. KOH solution. Scan rate: 5 mV s⁻¹; (d) comparison of electrochemical HER; the polarization curves were recorded before and after 10 000 CV potential cycles. Data taken from ref 68.

can offer a larger amount of catalytic active sites than their crystalline counterparts.⁶⁷

Kweon et al.⁶⁸ described an inexpensive and simple approach for producing homogeneous ruthenium (Ru) nanoparticles as an effective HER electrocatalyst by depositing Ru on multi-walled carbon nanotubes (MWCNTs) (Figure 5a). According to Figure 5b and Figure 5c, the synthesized electrocatalyst outperforms commercial Pt/C with low overpotentials of 13 and 17 mV at 10 mA cm⁻² in 0.5 M aq. H₂SO₄ and 1.0 M aq. KOH, respectively. Furthermore, the catalyst has exceptional stability in both media, revealing nearly zero during cycling (Figure 5d). In this study, DTF calculations indicate that Ru–C bonding is the most likely effective area for the HER.

In electrocatalysts, surface properties play a decisive role in intrinsic activity and adaptability. Bao et al.⁶⁹ demonstrated a simple approach for thermally doping Ru/C with atomically scattered cobalt atoms. The generated amorphous shell containing Ru–Co sites on the Ru/C electrocatalyst by a surface-engineering approach considerably increased HER activity and stability in this study. Similar to Pt/C but considerably better, the Co_xRu@Ru/CN_x electrocatalyst displayed an overpotential of 30 mV at 10 mA cm⁻². This excellent information shows that this obtained electrocatalyst is one of the best HER catalysts for the alkaline environment that has been proposed so far. The other way to reduce the loading of noble metals is to alloy them with inexpensive metals.⁷⁰ The ideal method is to utilize one or more metals that have an extra

favorable influence on the material's catalytic activity. Some Pt-based alloys can be made with Pt–M crystalline nanoparticles (M = Co, Fe, Cu, Ru, Au). In this method, we substitute inexpensive metals for Pt, intending to increase synergy and electrocatalytic performance. There are two key explanations for the improved performance of these materials over commercial Pt nanoparticle-based catalysts. The first explanation is the “effect of ligand”, which relates to the electronic characteristics of one transition metal's active sites close to another metal's active sites. Another reason is the “effect of lattice strain” on the Pt–Pt bond distance because of the mixture of other metals, which causes changes in the Pt metal's d-bond center.⁷¹ This factor can be changed by combining Pt with other metals in the network to provide the best catalyst properties. These findings were confirmed by other research groups.⁷² The ability to modify the structure on the surface is essential for enhancing electrocatalytic activity among various noble metal-based electrocatalysts for HER. Doping noble metal-based materials with other metal components has recently been discovered to be another efficient method of increasing the electrocatalytic activity of HER while minimizing the quantity of noble metal utilized. Electrochemical analysis of HER showed that doping, especially the combination of S and N in the noble metal, improves the electrocatalytic behavior and increases the stability. Naveen et al.⁷³ reported a Pd nanoparticles (NPs) electrocatalyst supported on a carbon sphere nanoarchitecture doped with sulfur (S) and nitrogen (N) atoms (PdSNC), which

is designed by using a palladium–rubeanic acid (Pd–RA) coordination polymer as a precursor, which was then calcined of materials for the HER electrocatalyst. Doping S and N into carbon structures increased the electronic structure and strengthened the affinity of the PdNPs in this study, revealing improved electrochemical performance of the electrocatalyst. By modulating the electronic structure and stabilizing Pd nanoparticles, the placement of dual heteroatoms (S and N) in carbon tissue enhanced stable electrocatalytic activity as an alternative to expensive commercial Pt/C. The modified PdSNC demonstrated a current of 10 mA cm⁻² at 0.030 V, which is significantly higher than Pd/C and comparable to Pt/C. This strategy used by researchers (doping and Pd/C formation) is a promising approach to designing carbon/noble metal composites with heteroatoms to enhance electrocatalytic performance. In electrocatalysts, surface properties play a decisive role in intrinsic activity and adaptability.⁷⁴ Noble metals provide exceptional benefits for water-splitting processes, but their high price and scarcity remain substantial barriers to broad industrial growth. It should also be mentioned that the usage of noble metals is required for many important applications.^{35,75} As a result, it is possible to infer that the most promising strategy, particularly for large-scale applications, is the creation of electrocatalysts based on cheap and readily available materials. The HER performances of PGM-free catalysts are summarized in Table 2.

4.2. Non-Noble Metal-Based Electrocatalysts. As summarized in the previous chapter, non-noble metal-based electrocatalysts are the only viable option for the future development of large-scale water splitting for energy conversion.

Table 2. HER Performance Summary of PGM-free Materials Catalysts

material	structure	Tafel slope (mV dec ⁻¹)	η (mV vs RHE) for $J = 10 \text{ mA cm}^{-2}$	refs
NiCoN	nitride	105.2	145	76
Ni ₃ N–NiMoN	nitride	64	31	77
MoSe ₂ /NiSe ₂	selenide	46.9	249 mV at 100 mA	78
Ni _{0.7} Co _{0.3} Se ₂	selenide	31.6	108	79
NiMoNx/C	nitride	35	78 mV at 100 mA	80
Mo–Fe–Se–CP	selenide	57.7	86.9	81
Ni ₃ N/VN–NF	nitride	47	56	82
Fe ₂ P/Fe	phosphide	55	191	83
CO ₂ P/CP	phosphide	60	174	83
CO ₂ P	phosphide	101	406	84
MO ₂ N/NC	nitride	115.7	217	85
FeP	phosphide	37	50	86
V ₈ C ₇ @GC NSs/NF	carbide	34.5	38	87
WN/CC	nitride	57.1	130	88
porous CoP ₂	phosphide	67	56	89
MoNx	nitride	114	148	90
VMoN	nitride	60	108	91
CoNiSe ₂ /NF	selenide	40	87	92
CoNiSe/NC	selenide	66.5	100	93
Mo ₂ C/C-900	carbide	52	114	94
nanoMoC@GS	carbide	43	124	95
MoN	nitride	120	389	96
WN–W ₂ C	nitride	85	242	97
NiCoP holey	phosphide	57	58	98
CoP ₂ /rGO	phosphide	50	88	99

According to the study, replacing noble metals with a combination of transition metals and nonmetal elements (S, Se, N, C, and P) has emerged as a potential alternative. Metal sulfides, metal selenides, metal nitrides, metal carbides, and metal phosphides might be mentioned in this group of transition metal-based electrocatalysts with high activity, stability, and affordable pricing.¹⁰⁰ The following sections summarize the most advanced electrocatalysts selected based on the most common materials and compare each group with Pt-based electrocatalysts.¹⁰¹ Mn, Fe, Co, and Ni are some of the most widely used non-noble metal electrocatalysts for HER. As an affordable metal with widespread industrial application and strong HER activity, take Fe as an example (at 10 mA cm⁻², the overpotential can reach the lowest value of about 260 mV).¹⁰² Fe is an inexpensive metal that is often employed in industrial settings and has comparatively high HER activity. Pure Fe is employed as a comparison material on occasion, and it can produce diverse findings depending on the preparation process, surface area, morphology, or shape.^{103,104} Unfortunately, there are not many studies done on pure iron as a cathode material. One factor might be the low stability of Fe alone in high-temperature, alkaline conditions. This instability is increased in the no-current mode when the electrolysis is switched off. The low stability and efficiency of Fe cathodes under water-splitting conditions can be reduced by alloying them with one or more metals.^{104,105} These objective characteristics are heavily influenced by the kind of coalloyed metal, overall composition, and preparation technique. Steel materials have historically been utilized as dual-function catalysts in overall water splitting, despite the fact that their catalytic activity, particularly for HER, is significantly inferior to that of the most sophisticated catalysts.¹⁰⁶ Surface modification appears to be a viable method for dramatically increasing the activity of steel-based materials.^{107,108} In one study, Kim et al.¹⁰⁸ studied a self-activated nanoporous anodic stainless steel electrode with better catalytic performance for the hydrogen evolution reaction.

Etched and anodized stainless steel (EASS) is created in this technique by employing etched 304 stainless steel foil with an uneven surface and then thermal annealing (650 °C, Ar and H₂ mixture, 1 h). The synthesis method increases the electrode's surface area, exposing a large number of active sites and oxygen vacancies. The improved material displayed an overpotential of 370 mV at 10 mA cm⁻², almost 100 mV less than the original stainless steel (466 mV). In addition, the overpotential is decreased to 244 mV by self-activation after 10 000 LSV cycles due to the creation of a catalytically active metal hydroxide layer on the surface of the electrode. Although significant progress has been made in this field, as far as we know, the most active steel-based electrocatalysts still need to be doped with more active substances, such as Ni, Mo, or P, to achieve an overpotential of only 80–120 mV higher than that observed with commercial Pt/C electrocatalysts.¹⁰⁹ In addition to stainless steel, the most researched iron-based alloys are the Fe–Co and Fe–Mo groups, which may be utilized as binary alloys or to complement another metal to produce a more complicated system. A high actual surface area Fe–Mo alloy is a potential material for HER.^{54–56}

4.2.1. Transition Metal Carbides. Transition metal carbides (TMCs) demonstrate Pt-like properties for HER electrocatalytic activity due to the shift in the d-band center; for this reason, the development of these electrocatalysts as non-noble metal-based electrocatalysts is of great interest.¹¹⁰ Group IVb–VIb TMCs are known as transition carbides due to the electronic properties of carbon atoms occupying the metal lattice's

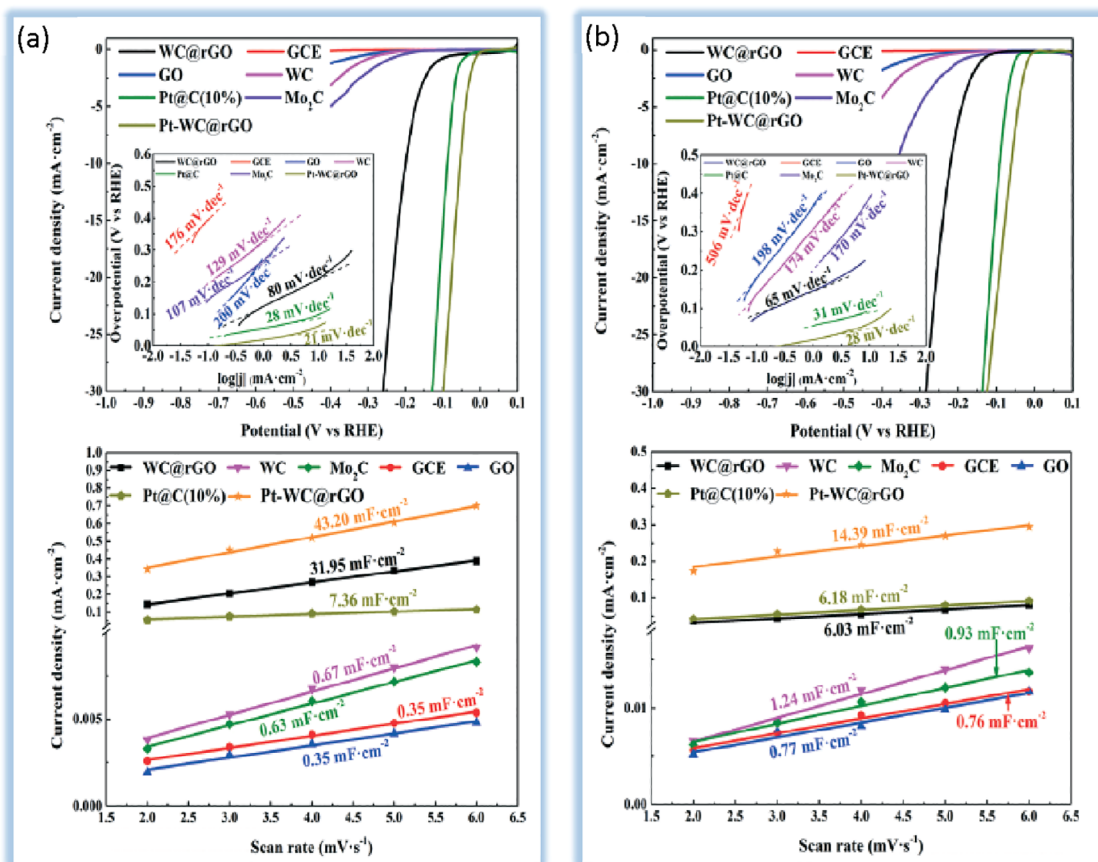


Figure 6. Polarization curves (inset: Tafel plots obtained from the polarization curves), calculated electrochemical double-layer capacitance, and η_{10} values of corresponding materials in (a) acidic solutions and (b) alkaline solutions. Data taken from ref 113.

position.¹¹¹ W and Mo are the most common candidates for use in TMCs, which in addition to high electrical conductivity, hydrogen adsorption properties, and d-band electron density state, create the optimal compound that can demonstrate near-Pt electrocatalytic activity for HER electrocatalysis.¹¹² WC is one of the first noble metal electrocatalysts for HER electrocatalysis. The W/C ratio substantially influences the electrocatalytic activity of HER in this combination. The electrocatalytic activity of WC, like that of other compounds, is determined by the number of active sites, crystalline phases, and nanoparticle morphology. Lv et al.¹¹³ adopted a simple approach to create WC@rGO in order to increase HER activity in both acidic and alkaline environments. In order to increase charge transfer and change the size of the WC particle in order to achieve effective and stable HER performance, this study employed the efficiently conductive rGO as a support. The overpotentials of the synthesized electrocatalyst are about 2.5 times smaller than those of the pristine WC to achieve 10 mA cm^{-2} in solutions (acidic and alkaline). As shown in Figure 6a and 6b, the Pt-modified WC electrocatalyst with low Pt accumulation (4% by weight) shows even heightened performance of the electrocatalyst (Tafel slope and η_{10} of 21 mV dec^{-1} and 54 mV in solution of acid and 28 mV dec^{-1} and 61 mV in solution of alkaline) to commercial Pt/C. The author's method makes it possible to prepare environmentally friendly, inexpensive, stable, and effective HER electrodes.

It is worth noting that the surface of the electrocatalyst must be free of tungsten oxide or similar compounds to achieve the flawless electrocatalytic activity, as the oxygen species in

tungsten carbon disrupt the active sites in the HER electrocatalyst reaction. This is in contrast to transition metal chalcogenides in which the presence of oxygen can improve HER performance. In the interaction of the electrocatalyst with water, the WC surface disrupts and inactivates the formation of a WO_3 layer.¹¹⁴ Although this oxide layer grows at anodic potentials, it should not be present at HER cathodic potentials. Also, its stability in anodic potentials is shallow due to the formation of an anodizing layer. Due to the synergistic effect between WC and Pt, more attention has been focused on using this material as a substrate for Pt electrocatalysts, although its mechanism is still unknown.¹¹⁵ Researchers are currently focusing on reducing the Pt content of Pt/WC electrocatalysts with low cost, high efficiency, and good stability for HER.

Mo_2C also has Pt-like electrocatalytic activity for the HER. In addition, a comparative study showed that molybdenum carbide had better electrocatalytic performance than nitride and boride.¹¹⁶ Liu et al.¹¹⁷ used CO_2 as the feedstock to create a self-standing $\text{MoC}-\text{Mo}_2\text{C}$ catalytic electrode. High performance of the synthesized electrode with low overpotential at 500 mA cm^{-2} was observed in both acidic and alkaline mediums (256 and 292 mV , respectively), due to its hydrophilic porous surface and inherent mechanical strength, the long-lasting lifetime of more than 2400 h , and performance at high temperatures ($70 \text{ }^\circ\text{C}$). By DFT calculations, the authors show that the superior performance of the HER discontinuous carbide electrode in both acidic and alkaline states is determined by the heterogeneous bonding of $\text{MoC}(001)-\text{Mo}_2\text{C}(101)$ with $\Delta G_{\text{H}^*} = -0.13 \text{ eV}$ in acid.

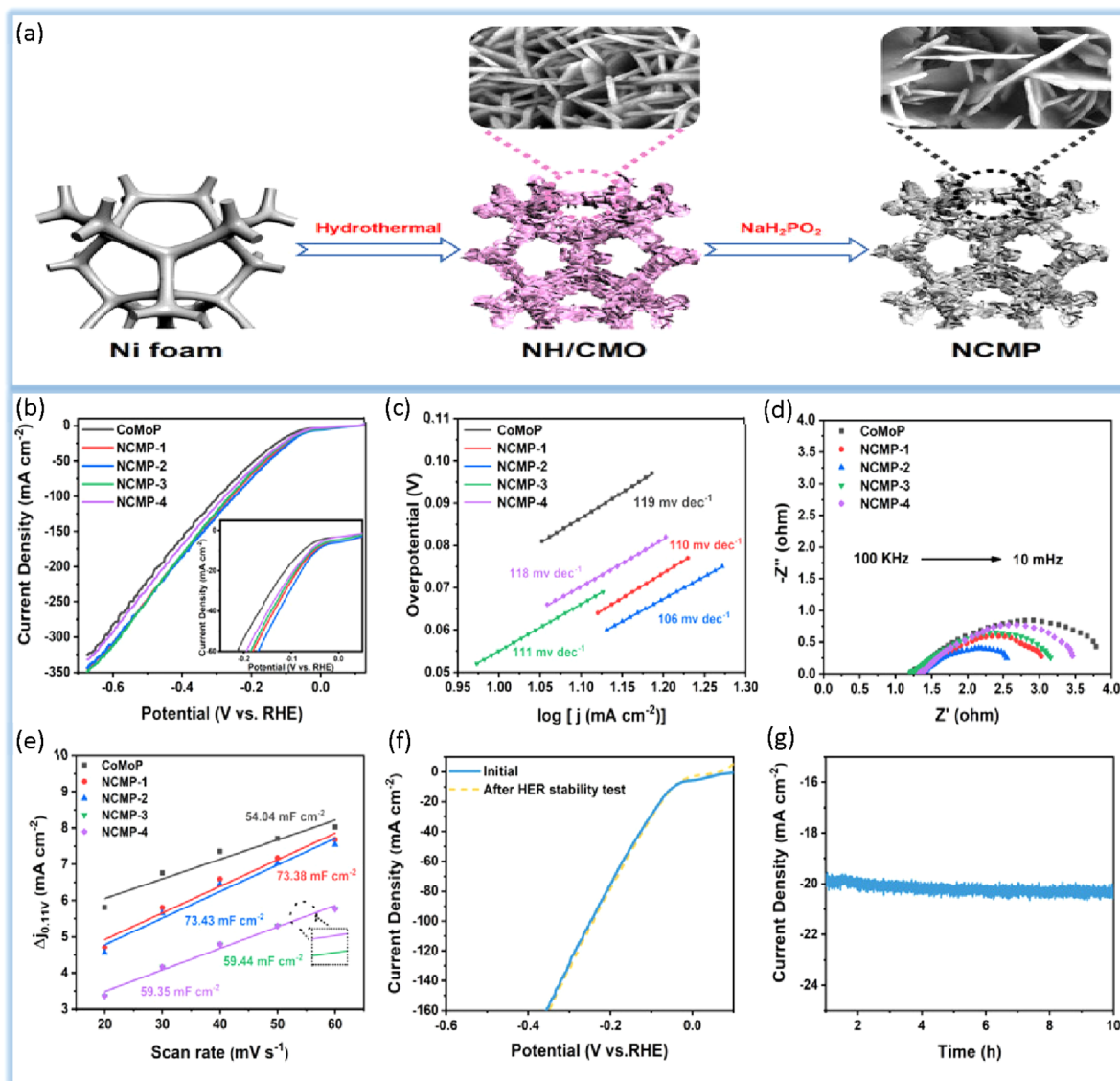


Figure 7. (a) Schematic Illustration of the formation process of NCMP. (b) HER polarization curves of NCMP- x ($x = 1, 2, 3,$ and 4) and CoMoP in 1 M KOH; inset: partial enlargement of (b). (c) Corresponding Tafel plots. (d) Nyquist plots of NCMP- x ($x = 1, 2, 3,$ and 4) and CoMoP. (e) Corresponding Cdl of CoMoP and NCMP- x ($x = 1, 2, 3,$ and 4) at 0.11 V vs reversible hydrogen electrode (RHE). (f) Polarization curves of NCMP-2 before and after 10 h test. (g) Long-term stability of NCMP-2 at a constant overpotential for 10 h in 1 M KOH. Data taken from ref 123.

The Mott–Schottky phenomenon between a metal with a higher work function and an n-type semiconductor with a greater Fermi level will make electron transmission from the semiconductor to the metal easier. As a consequence, designing optimum H^* adsorption active sites using ΔG_{H^*} is a possibility. Ji et al.¹¹⁸ reported that carbonization was used to create MoC nanoparticles embedded in N, P-codoped carbon from polyoxometalates and polypyrrole nanocomposites. Based on an increase in carrier density and an increase in electron transfer rate in MoC after reducing the work function due to the Mott–Schottky effect with n-type domains in N, P-codoped carbon, synthesized electrocatalysts can lead to a current density of 10 mA cm^{-2} at 175 mV with a Tafel slope of 62 mV dec^{-1} . In addition, the TOF value at 150 mV is 1.49 s^{-1} , as is the long-term stability of H_2 generation. Metal carbides are a promising choice for HER catalysts in alkaline conditions due to their low cost, high frequency, and the ability of obtaining alkaline activity approaching that of Pt. Regardless of its distinguishing characteristics, the durability of this class of catalysts during

intermittent operation remains a critical concern since carbon-based materials are naturally prone to corrosion, even under mild oxidative circumstances. As a result, it is proposed that future study in this field concentrates on strengthening the stability under anodic polarization that can occur after the electrolyzer is turned off.¹¹⁹

4.2.2. Transition Metal Phosphides. Transition metal phosphides (TMPs), due to their inherent activity and high stability in both acidic and alkaline environments, have presented themselves as potential candidates for HER electrocatalysis.¹²⁰ In TMPs' structure, the P atom plays an essential role in electrocatalytic activity due to its excellent conductivity and unique electronic structure. One of the reasons for the superiority of metal phosphides is that the activity of these compounds is not limited to the crystal edge sites. However, HER can also occur in bulk materials. In the TMPs, Ni- and Co-based phosphides are among the lucky members of this group for HER. Computational studies and empirical evidence have always suggested that NiP_x alloys are potential candidates for

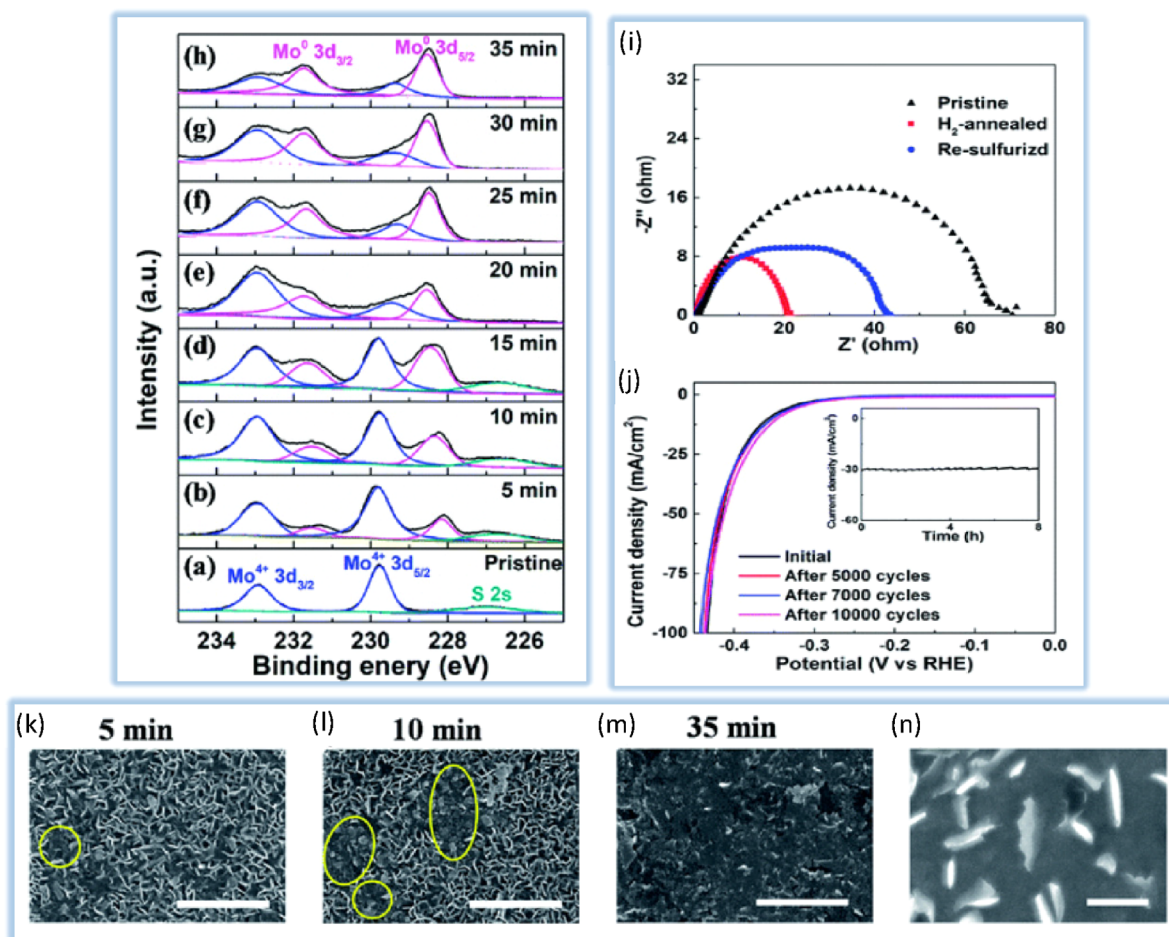


Figure 8. XPS data of the Mo 3d region for (a) pristine and H₂-annealed vertical MoS₂ nanosheets for (b) 5, (c) 10, (d) 15, (e) 20, (f) 25, (g) 30 and (h) 35 min, respectively. (i) EIS of pristine, H₂-annealed, and resulfurized vertical MoS₂ nanosheets. All of the spectra were collected by scanning from 0.1 to 106 Hz with an overpotential of 0.3 V. (g) Cathodic polarization curves of the H₂-annealed MoS₂ for 20 min before and after 5 000, 7 000, and 10 000 cycles, respectively. Inset: time-dependent current density of the H₂-annealed MoS₂ for 20 min under a static overpotential of 400 mV for 8 h. (k–n) SEM images of H₂-annealed vertical MoS₂ nanosheets for 5, 10, and 35 min, respectively; scale bar: 1 μm. (d) High-magnification SEM image of H₂-annealed vertical MoS₂ nanosheets for 20 min, showing rough edges induced by H₂ annealing; scale bar: 200 nm. Data taken from ref 129.

HER electrocatalysis.¹²¹ Zhang et al.¹²² discovered a multiphase nickel phosphide electrocatalyst composed of porous nickel powder as a matrix with manganese doped into porous nickel powder containing phosphorus powder. After a high-temperature phosphating operation, a multiphase nickel phosphide electrocatalyst (Ni₃P, Ni₂P, Ni₁₂P₅) (Mn–NiP) was fabricated with a bimetallic compound. Transition metal phosphides are thought to be affordable and excellent HER catalysts. The activity of the doped catalyst with the right quantity of manganese has risen due to the regulatory influence of doped manganese on the electronic structure of nickel and the electronic contact among nickel and phosphorus. The evolutionary activity of 3Mn–NiP hydrogen in the whole pH range showed outstanding results. The overpotentials required to produce a current density of 10 mA cm⁻² of 3Mn–NiP were 164 and 77 mV at acidic and alkaline solutions, respectively. Wang et al.¹²³ demonstrated a one-step hydrothermal method for synthesizing NiP₂ with CoMoP nanosheets (NCMP) under low-temperature phosphidation conditions. In the synthesized electrocatalyst, the synergistic effect of two different components, NiP₂ and CoMoP, is induced. In this study, to find the superior catalyst, the effect of nickel content on the performance of the catalyst is also studied, and it is found that when the nickel

dose is 0.02 mM, it shows the most prominent overpotentials of 46 mV at 10 mA cm⁻². It should be noted that the phosphides of the transition metals are reactive due to the negatively charged P-sites. As a result of this reactivity, a passive layer can quickly form on the electrocatalyst surface, which can completely disrupt the electrocatalytic reaction. Studies have shown that even shallow doses of NiP₂ can effectively improve the HER performance (Figure 7).

4.2.3. Transition Metal Chalcogenides (Sulfides and Selenides). Transition metal chalcogenides, relying on properties such as being inexpensive and ease of preparation, are promising candidates to replace noble metals for HER. According to the existing studies, metal selenides show higher catalytic activity than other members of the chalcogenides.^{48,124} The structures of metal sulfides are more straightforward than those of metal electrocatalysts, and their structure must be carefully adjusted for efficient HER operation.¹²⁵ Contrary to popular belief, metal sulfides are not vulnerable to the sulfur position. It is worth noting that these electrocatalysts can perform well in low H coatings, but their electrical conductivity decreases significantly with increasing H coating.¹²⁶

The shortage of highly efficient and inexpensive catalysts severely hinders the spread of HER on a large scale. Among

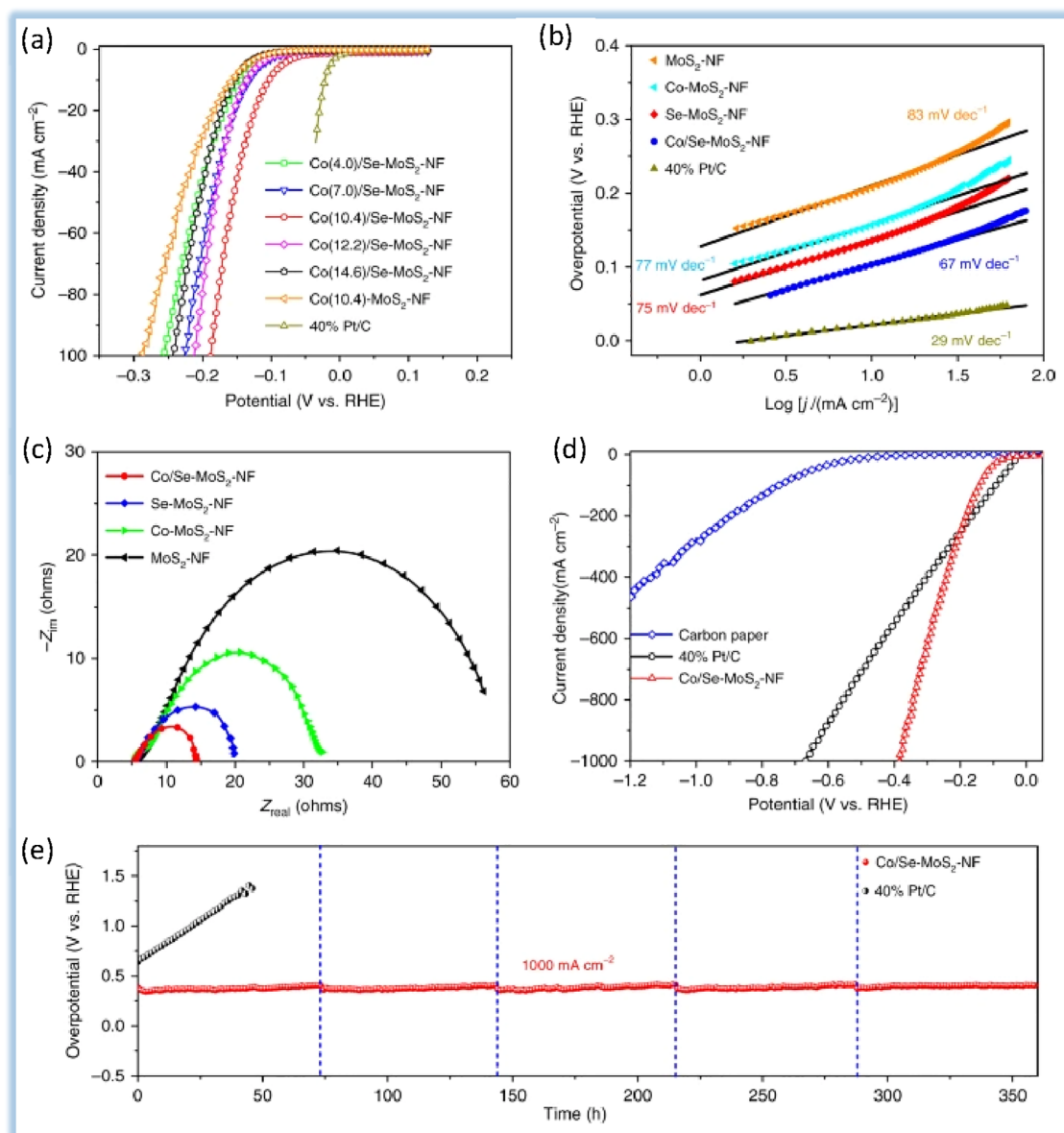


Figure 9. (a) HER polarization curves for Co/Se–MoS₂–NF with different Co-doping contents in comparison with Co–MoS₂–NF and 40% Pt/C. All samples are drop-casted on glassy carbon electrode for measurements. The Tafel plots (b) and the electrochemical impedance spectroscopy (EIS) Nyquist plots (c) of Co/Se–MoS₂–NF sample compared with Co–MoS₂–NF, Se–MoS₂–NF, MoS₂–NF, and commercial 40% Pt/C. (d) HER polarization curves for Co/Se–MoS₂–NF under large current densities in comparison with 40% Pt/C and carbon paper. Co/Se–MoS₂–NF and 40% Pt/C are drop-casted on carbon paper for measurements. (e) Chronopotentiometric measurements of long-term stability for Co/Se–MoS₂–NF and 40% Pt/C at 1000 mA cm⁻². The vertical dotted lines in (e) mark the time span (every 72 h) of replacing the electrolyte in the 360 h chronoamperometry test. All the HER measurements were conducted in a 0.5 M H₂SO₄ electrolyte at 25 °C. Data taken from ref 131.

metal sulfides, molybdenum sulfide is one of the most common candidates for HER electrocatalysts due to its cheapness and flexibility in design.¹²⁷ It can be considered a pioneer in this group of electrocatalysts. In the MoS₂ electrocatalyst, only the edges and voids S are the active catalytic sites for HER. Therefore, to increase the electrocatalytic activity, it is very important to increase and improve the structure of the edge sites and the S-vacancy.¹²⁸ He et al.¹²⁹ demonstrated HER activity enhancement by combining vertical nanosheets with H₂ annealing in a modified MoS₂. Due to a greater number of edges, horizontal MoS₂ nanosheets with this structural alteration demonstrated stronger HER activity than pure vertical MoS₂ nanosheets. In justifying the increase in electrocatalytic properties, it should be said that H₂ annealing further enhanced

the HER activity of vertical MoS₂ nanosheets remarkably. According to Figure 8, XPS results show a minor S:Mo ratio after H₂ annealing, indicating increased S-vacancy. In the meanwhile, EIS measurements demonstrate that H₂ annealing speeds up load transfer. SEM images show that H₂ annealing roughens the edges of MoS₂ and creates more edge sites, which improves the electrocatalyst behavior for HER.

In an ideal structure, MoS₂ is a 2D network with six S atoms around each Mo atom in an octagonal configuration. MoS₂ alone suffers from low catalytic performance for HER.^{1,130} Zheng et al.¹³¹ proposed a triple-layer MoS₂ nanofoam structure that encloses the surface selenium and cobalt in the inner layer, whose HER activity is higher than all reported heteroatom-doped MoS₂. As shown in Figure 9, the Co/Se–MoS₂–NF

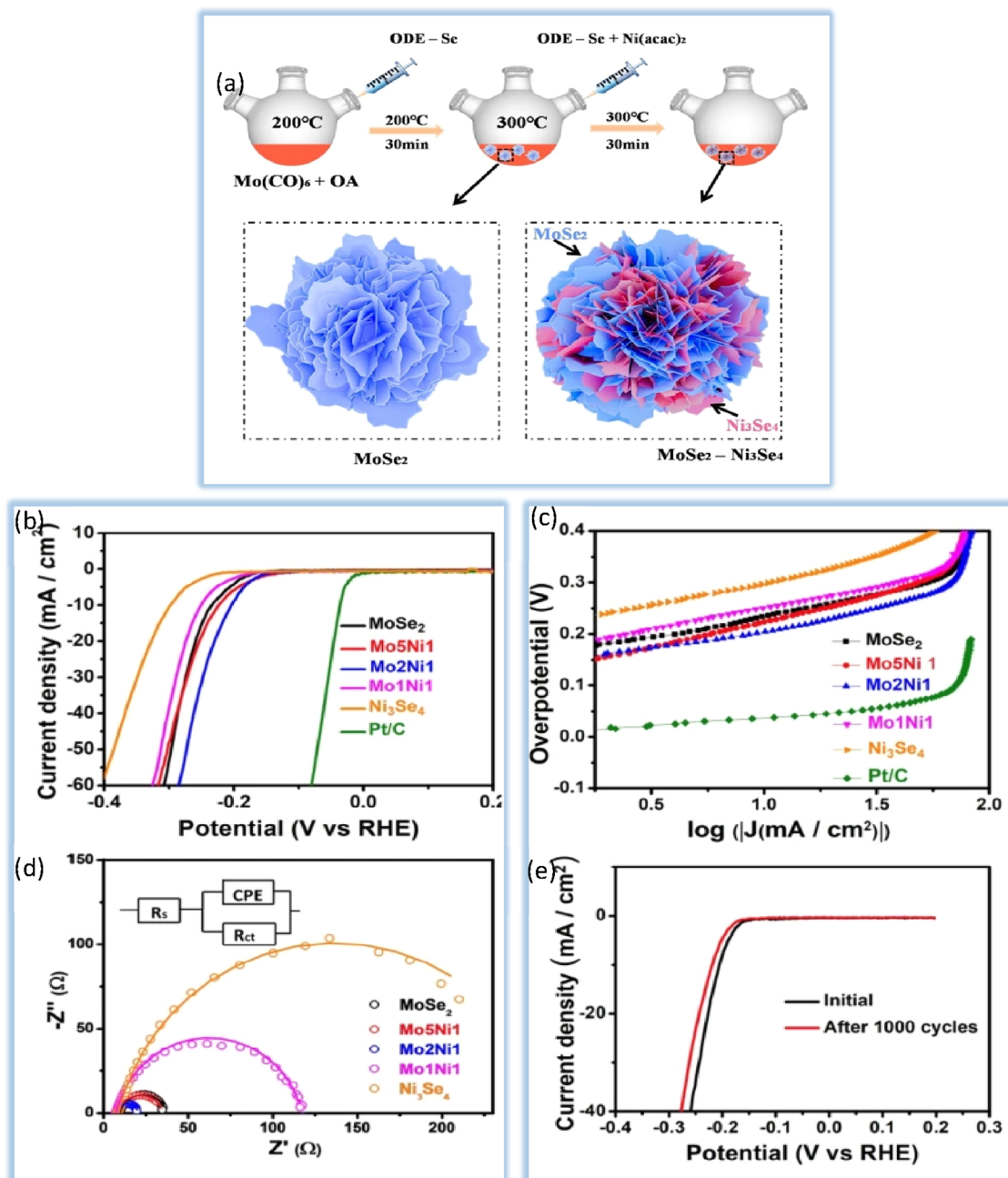


Figure 10. (a) Schematic diagram of the formation of $\text{MoSe}_2\text{-Ni}_3\text{Se}_4$ hybrid nanoelectrocatalysts. Polarization curves (b) and corresponding Tafel plots (c) of MoSe_2 , Mo_5Ni_1 , Mo_2Ni_1 , Mo_1Ni_1 , Ni_3Se_4 , and Pt/C. (d) Nyquist plots at an overpotential of 250 mV. (e) Polarization curves of a Mo_2Ni_1 sample before and after 1000 cycles. Data taken from ref 139.

synthesized sample exhibits a much lower overpotential of 382 mV than that of 671 mV over commercial Pt/C catalyst at a high current density of 1000 mA cm^{-2} . Also, the high activity can remain stable with the long-term stability of more than 360 h without destruction. According to this study, structure engineering of MoS_2 via confining multielements proposal is a promising and feasible way of developing high-performance and low-cost MoS_2 electrocatalysts for large-scale HER. DFT calculations show that the Co atoms enclosed in the inner layer of the structure excite the adjacent S atoms. In contrast, the Se atoms enclose the surface of the structure, which allows the creation of comprehensive active sites inside the plate and edge with optimal hydrogen adsorption activity. The strategy in question provides a viable pathway for developing MoS_2 -based

catalysts for industrial hydrogen production applications. In this study, Figure 9a shows the HER polarization curves of the Se-doped MoS_2 nanofoam ($\text{Se-MoS}_2\text{-NF}$) with different Se-doping contents and Co/Se-codoped MoS_2 nanofoam ($\text{Co/Se-MoS}_2\text{-NF}$) with different Co-doping contents. The onset overpotentials for delivering current densities of -10 and -100 mA cm^{-2} in $0.5 \text{ M H}_2\text{SO}_4$ electrolyte at 25°C are plotted for comparison. The $\text{Se-MoS}_2\text{-NF}$ sample with 9.1% Se-doping content exhibits the lowest onset overpotentials for both current densities, indicating the highest HER activity. This is because Se doping introduces more edge sites in the MoS_2 nanoflakes, which are more active for HER. As the Se-doping content increases from 9.1% to 14.6%, the HER activity gradually decreases. This is because excessive Se doping may lead to the

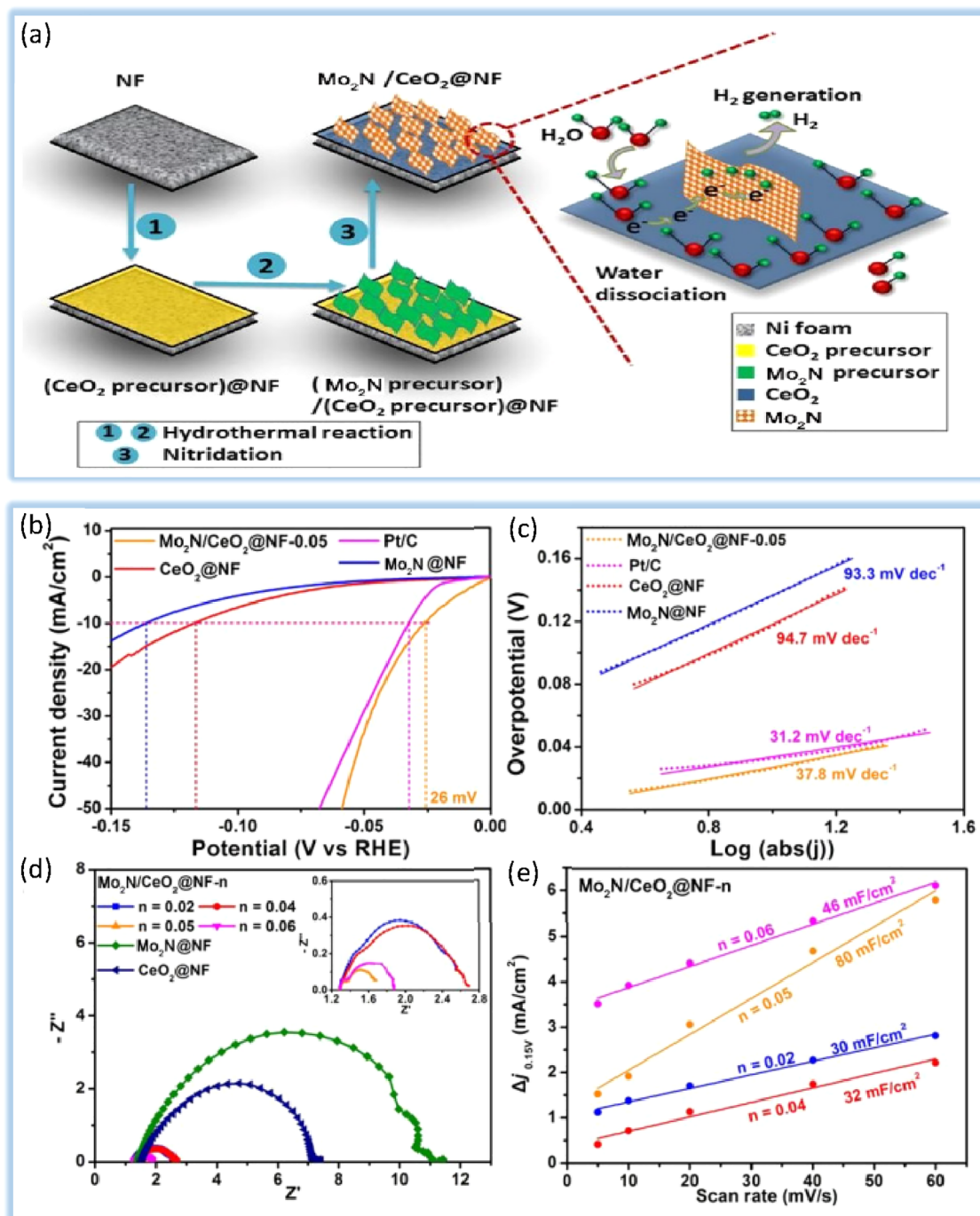


Figure 11. (a) Schematic illustration of the fabrication process of Mo₂N/CeO₂@nickel foam and the catalytic process. (b) Current vs overpotential plots for Mo₂N/CeO₂@NF-0.05, CeO₂@NF, Mo₂N@NF, and Pt/C. (c) Tafel plots for Mo₂N/CeO₂@NF-0.05, CeO₂@NF, Mo₂N@NF, and Pt/C. (d) Nyquist plots for Mo₂N/CeO₂@NF-*n* (*n* = 0.02, 0.04, 0.05, and 0.06), CeO₂@NF, and Mo₂N@NF. Inset, enlarged view of Nyquist plots for Mo₂N/CeO₂@NF-*n* (*n* = 0.02, 0.04, 0.05, and 0.06). (e) Current density as a function of scan rate of various electrodes, where the slope represents Cdl. Data taken from ref 144.

formation of overcoordinated S atoms with weakened adsorption of H* at the edge sites. The Co/Se–MoS₂–NF sample with 10.4% Co-doping content exhibits the lowest onset overpotentials for all three current densities, indicating the highest HER activity. This is because Co doping promotes the formation of more edge sites and also enhances the electronic conductivity of the catalyst. Figure 9b shows the Tafel slopes of the HER polarization curves of the Se–MoS₂–NF and Co/Se–MoS₂–NF samples. The Tafel slope is a measure of the rate of

electron transfer in the HER reaction. A lower Tafel slope indicates a faster rate of electron transfer, which means a more efficient catalyst. The Co(10.4)/Se–MoS₂–NF sample exhibits the lowest Tafel slope of 67 mV dec⁻¹, which is significantly lower than the Tafel slopes of the Se–MoS₂–NF (75 mV dec⁻¹), Co(10.4)–MoS₂–NF (77 mV dec⁻¹), and undoped MoS₂–NF (83 mV dec⁻¹) samples. This clearly demonstrates the superior HER kinetics of the Co/Se-codoped MoS₂ catalyst. Also, Figure 9c shows the results of electrochemical impedance

spectroscopy (EIS) measurements of the Se–MoS₂–NF and Co/Se–MoS₂–NF samples. EIS measurements are used to measure the charge transfer resistance (R_{ct}) of a catalyst, which is a measure of the intrinsic resistance to electron transfer. A lower R_{ct} value indicates a more efficient catalyst. The Co(10.4)/Se–MoS₂–NF sample exhibits the lowest R_{ct} value of all the samples, which confirms that it is the most efficient HER catalyst.

Fractal-shaped MoS₂ has been shown to exhibit enhanced hydrogen evolution reaction (HER) performance compared to its planar counterpart. This is attributed to the increased number of edge sites, which are the active sites for HER. The fractal morphology of MoS₂ can be induced by nonequilibrium growth conditions, such as rapid heating rates and high Mo precursor concentrations. The enhanced HER activity of fractal MoS₂ can be attributed to the increased number of edge sites. Edge sites are more reactive than basal plane sites due to their higher exposure to the electrolyte. The higher reactivity of edge sites is due to the weaker bonding between edge atoms and the MoS₂ lattice. This weaker bonding allows edge atoms to more easily dissociate hydrogen from water molecules. The fractal morphology can be induced by nonequilibrium growth conditions, and the enhanced activity can be attributed to the increased number of edge sites and the higher surface area.¹³² Like metal sulfides, the metal selenides have attracted much attention in the past decade. Because the intended reaction only occurs on the crystal's edges, selenides' electrocatalyst activity is greatly determined by the amount of active sites on its surface.¹³³ Therefore, catalyst surface optimization seems to be critical for creating active and enriched edge locations. In general, metal selenides, like metal sulfides, follow a similar route due to their propensity to function as an active catalyst for HER in an alkaline environment.¹³⁴ Aside from surface modification, combining a metal selenide with another group(s) (such as phosphides or sulfides) can have a significant impact on the electrocatalyst's efficiency.¹³⁵ The strategy of this method is based on increasing the number of active sites in the electrocatalyst, which leads to increased electrode activity. MoSe₂ is considered a promising electrocatalyst for the HER to produce green energy due to its availability and low preparation cost.¹³⁶ Applicable structural changes in the building of this MoSe₂ can significantly improve its efficiency.¹³⁷ In the past decade, the use of 2D structures and hybrid nanoelectrocatalysts for HER has emerged as efficient and cost-effective electrocatalysts. A MoSe₂ hybrid with other transition metal dichalcogenides to form an optimal nanostructure is an effective way to increase HER electrocatalytic activity to replace a Pt electrocatalyst.¹³⁸ Wu et al.¹³⁹ adopted a seed-induced solution technique to create MoSe₂–Ni₃Se₄ hybrid nanoelectrocatalysts with a flowerlike shape (Figure 10). In the structure, the Ni₃Se₄ component instinctively tends to nucleate instead of independent nucleation to form individual nanocrystals, growing on the surfaces of very thin MoSe₂ nanoparticles to form an efficient hybrid nanostructure. The HER catalytic activities of MoSe₂–Ni₃Se₄ hybrid nanoelectrocatalysts with varied Mo:Ni ratios are compared. The comparison of MoSe₂–Ni₃Se₄ hybrid nanoelectrocatalysts with varied Mo:Ni ratios reveals that Mo:Ni ratios impact HER activities. The MoSe₂–Ni₃Se₄ hybrid has a Mo:Ni molar ratio of 2:1 and increased HER characteristics, with a Tafel slope of 57 mV dec^{−1} and an overpotential of 203 mV at 10 mA cm^{−2}. It should be noted that only the triangular prism phase edge locations have HER electrocatalytic properties and the base plate, which usually does not have defective/unsaturated locations, is inactive. In addition to the alkaline

medium, metal selenides have been successfully tested in acidic media.

4.2.4. Transition Metal Nitrides. Transition metal nitrides (TMNs), known as transition alloys, have recently been proposed as efficient HER electrocatalysts as alternatives to noble metal electrocatalysts due to their exceptional electrical conductivity, corrosion resistance, mechanical robustness, and high electrochemical stability.¹⁴⁰ Metal nitrides are particularly appealing for future investigation due to their exceptional properties. Direct nitridation is the traditional way of producing metal nitrides. Heating an NF (nickel foam) in an NH₃ atm, for example, can provide an active Ni₃N/Ni foam electrocatalyst with exceptional qualities (overpotential 121 mV at 10 mA cm^{−2} and even stable in an alkaline environment, 1 M KOH, 32 h).¹⁴¹ TMNs containing Mo or Ni can achieve Pt-like activity in alkaline environments.^{142,143} Wang et al.¹⁴⁴ published a self-supporting electrocatalyst preparing the growth of a MO₂N layer on a CeO₂ layer deposited on NF. According to Figure 11a, the synthesized MO₂N/CeO₂@NF showed an attractive catalytic activity for the HER at 1.0 M KOH even more efficiently than the Pt/C electrode and relatively low overpotential of 26 mV for a current density of 10 mA cm^{−2}. The stability of this electrocatalyst for a long time (24 h) was also evaluated. The results offer great hope for building an inexpensive and stable TMNs electrocatalyst for a water-splitting reaction.

This study discusses the current density versus overpotential plots (Figure 11a) obtained from linear sweep voltammetry (LSV) measurements. It compares the HER activities of different electrodes, including Pt/C, CeO₂@NF, Mo₂N@NF, and Mo₂N/CeO₂@NF-*n*. The text highlights the overpotentials and current densities at 10 mA/cm² for each electrode, demonstrating the performance of Mo₂N/CeO₂@NF-0.05 as the electrode with the smallest overpotential for HER in alkaline solution, comparable to Pt. Authors provides Tafel plots (Figure 11b) to analyze the kinetics of the HER for the different electrodes. The Tafel slopes obtained from these plots are compared, with Mo₂N/CeO₂@NF-0.05 and Pt/C showing smaller slopes than CeO₂@NF and Mo₂N@NF. This comparison suggests that Mo₂N/CeO₂@NF-0.05 is as efficient as the Pt electrode for HER in alkaline solution. Additionally, this report includes Nyquist plots (Figure 11c) obtained from electrochemical impedance spectroscopy (EIS) measurements. The analysis of the Nyquist plots indicates that Mo₂N/CeO₂@NF-0.05 exhibits the fastest electron transfer in the HER process, as reflected by the smallest semicircle radius. This observation aligns with the electrode's lowest Tafel slope and suggests that Mo₂N/CeO₂@NF-0.05 has the best HER activity among the different Mo₂N/CeO₂@NF-*n* electrodes.

The fabrication of Ni-based electrode materials has attracted much attention due to their suitable activity and good stability to replace expensive Pt for producing molecular hydrogen through the electrolysis of water. Supporting elements such as carbon are commonly utilized in this context to boost electrical conductivity and catalytic activity. Balaji et al.¹⁴⁵ observed a particular pathway for fabricating carbon-backed Ni₃N/Ni as an efficient HER electrocatalyst in both 0.5 M H₂SO₄ and 1 M KOH environments. By providing intrinsically active sites, carbon support can effectively enhance the electronic structure of Ni₃N/Ni. Superior electrical conductivity and charge transfer rate are demonstrated by the optimized Ni₃N/Ni@C electrocatalyst. The TMNs composite also showed improved electrocatalytic behavior with a low overpotential of 163 and 172 mV at 10 mA cm^{−2} and durability over 1000 cycles in acidic and

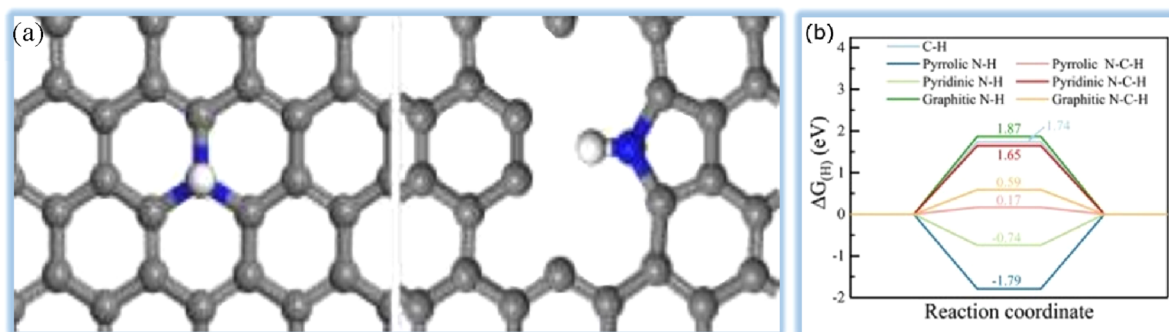


Figure 12. (a) Heteroatom-doping process on graphitic carbon. (b) Nitrogen-doped vertical graphene as a metal-free catalyst for HER exhibits a good activity and an excellent stability, which can be ascribed to the optimization of $\Delta G_{(H)}$ by N doping and the robust structure of VG. Data taken from ref 159.

alkaline solutions for HER application. In TMNs, the density of states in the d-band of the corresponding metal is regulated by the nitrogen atom.^{143,146} Therefore, there is a minor deficiency in the occupation of the d-band. In this respect, they can compete with TMCs. An exciting feature of TMNs is that they can be used in alkaline environments with high stability.

Kamran et al. reported the development of a novel nanoheterostructured catalyst for the HER in alkaline electrolytes. The catalyst, $\text{Ni}(\text{OH})_2@\text{Ni-N/Ni-C/NF}$, is composed of $\text{Ni}(\text{OH})_2$ nanoparticles embedded in an outer layer of Ni-N/Ni-C. The nanoheterointerfacial between $\text{Ni}(\text{OH})_2$ and Ni-N/Ni-C phases is shown to enhance the HER activity significantly compared to monophasic $\text{Ni}(\text{OH})_2$. The authors attribute the enhanced HER activity to the interphasic synergy between $\text{Ni}(\text{OH})_2$ and Ni-N/Ni-C phases. $\text{Ni}(\text{OH})_2$ is a strong water-splitting promoter, but it has a strong affinity for hydrogen, which hinders the hydrogen evolution process. Ni-N/Ni-C phases, on the other hand, have labile electronic properties and can facilitate the dissociation of hydrogen from adsorbed hydrogen species. The nanoheterointerfacial between $\text{Ni}(\text{OH})_2$ and Ni-N/Ni-C phases allows for the efficient transfer of electrons from $\text{Ni}(\text{OH})_2$ to hydrogen species on Ni-N/Ni-C phases, leading to enhanced HER activity. The authors demonstrated the superior performance of $\text{Ni}(\text{OH})_2@\text{Ni-N/Ni-C/NF}$ by comparing its HER activity to that of monophasic $\text{Ni}(\text{OH})_2$ and other benchmark catalysts. $\text{Ni}(\text{OH})_2@\text{Ni-N/Ni-C/NF}$ exhibited the lowest overpotentials for delivering current densities of -10 and -100 mA cm^{-2} in 1 M KOH compared to monophasic $\text{Ni}(\text{OH})_2$ and other catalysts. The Tafel slope of $\text{Ni}(\text{OH})_2@\text{Ni-N/Ni-C/NF}$ was also lower than that of monophasic $\text{Ni}(\text{OH})_2$, indicating a faster reaction rate. This work further demonstrated the stability of $\text{Ni}(\text{OH})_2@\text{Ni-N/Ni-C/NF}$ in alkaline electrolytes by subjecting it to cyclic voltammetry (CV) and chronopotentiometry (CP). $\text{Ni}(\text{OH})_2@\text{Ni-N/Ni-C/NF}$ exhibited good stability during CV and CP, with minimal degradation over time.¹⁴⁷

4.3. MOF-Based Electrocatalysts. The use of metal-organic frameworks (MOFs) in electrocatalytic, photocatalytic, and chemocatalytic processes makes them a strong choice for extremely effective HER.¹⁴⁸ Research on MOF-based HER catalysts involves a wide range of porous materials including as zeolite, polymer, carbon, and composite materials.¹⁴⁹ These species have evolved porosity with high specific surface area, flexible crystalline porous frameworks, and big pore volume, which is the primary property of their applicability in the HER process. Aside from the intrinsic features indicated, external changes to the main MOFs, such as the loading of active

nanoparticles and the bonding of functional surface species, are useful in increasing the activity of the catalysts.¹⁵⁰ However, MOF-based catalysts are more attractive and diverse than other types of porous catalysts due to the various compounds of metal centers and organic ligands. These compounds, like most other porous catalysts, can be utilized in “pristine”, “precursor”, or “derived” forms for the dispersion or separation of active catalytic species added to porous networks. According to research studies, the combination of nanoparticles and MOF compounds can produce amazing synergistic effects that lead to much better performance for the HER.¹⁵¹

As mentioned, electrocatalytic HER is usually achieved by establishing an electrical current due to a potential difference through an aqueous electrolyte to produce O_2 at the anode through the OER process and produce H_2 at the cathode side through the HER process. The half-reaction at the cathode side is the focus of most electrocatalytic HER research. However, in the case of water splitting, the performance of MOF-based catalysts at HER and OER must be compared.¹⁵² MOFs are frequently employed as supports or precursors; MOF-based derivatives or composite materials may retain the original MOF's porous structure, but the pore volume and specific surface area are decreased. Reduced porosity in MOF derivatives is caused by the collapse of the crystalline porous structure caused by breaking coordination bonds and eliminating noncarbon components at high temperatures.¹⁵³ When MOF is utilized as a support, it usually results in the colonization of pores by guest particles.¹⁵⁴ The reduction in porosity in this example is proportional to the size and dispersion of the guest particles.¹⁵⁵

However, the performance of MOF derivatives is not always compromised by lower porosity. It is important to note that MOF heat treatment is frequently used to produce MOF derivatives with particular chemical makeups and structures, such as metal oxides, metal carbides, metal nitrides, and metal sulfides. Yan et al.¹⁵⁶ synthesized nickel-cobalt bimetallic phosphide nanotubes from MOF-74- Co_2Ni , bimetallic for electrocatalytic water distribution. The specific surface area of pristine MOF reduced from 1100 to $55.6 \text{ m}^2 \text{ g}^{-1}$ after oxidation and phosphorylation. Encapsulation of guest molecules, on the other hand, tries to add more catalytically active sites into the original MOF or to increase the synergy between guest molecules and host materials. In 2017, Hao et al.¹⁵⁷ published the introduction of MoS_2 quantum dots and graphene into UiO-66- NH_2 (Zr-containing MOF) for HER. The specific surface area of the original MOF is $712.3 \text{ m}^2 \text{ g}^{-1}$, which decreases to about $457.24 \text{ m}^2 \text{ g}^{-1}$ after loading MoS_2 (5.0% by weight) and

graphene. Zhen et al.¹⁵⁸ improved the Ni nanoparticle-loaded MOF-5. After synthesis, due to the much-dispersed nanoparticles, the corresponding specific surface area reduced slightly (from 2973 to 2961 m² g⁻¹). These MOF-based materials mentioned above perform better in HER catalysis than their primary precursors (Figure 12).

5. SUMMARY AND PERSPECTIVES

Hydrogen is a favored alternative to fossil fuels since it has the highest gravitational energy density and produces no pollution, making it a clean and sustainable energy source. In the meanwhile, establishing water-dividing cells as an energy-efficient conversion mechanism is critical to hydrogen generation. However, due to the sluggish reaction kinetics of the OER and HER for the high overpotential, the energy efficiency of water electrolysis is low, and its practical use is hampered. HER is most likely the simplest and most direct method of producing high-quality and selective hydrogen. Pt has long been a suitable HER electrocatalyst, but its limited supplies and high cost make developing HER impracticable. Furthermore, since Pt must be utilized in combination with a carbon catalyst support, the mechanical stability of the electrocatalyst is a feature that might raise operating expenses. Pt recycling is another issue that plagues Pt-based systems. As a result, a shift in the approach of classic electrocatalysts appears to be unavoidable. However, enhancing present Pt electrocatalysts as a solution can drastically lower operating expenses. Practical methods for HER electrocatalysts have recently been established using non-noble metals and related compounds. To assist the practical use of water distribution in enterprises, the design of effective catalysts is critical in OER and HER to limit possible overcapacity, boost stability, and improve efficiency. The most common electrocatalytic activity parameters, such as overpotential at constant current density (10 mA cm⁻²) and Tafel slope, along with at least one of the classical stability tests, were selected as the main comparison parameters. The main parameters affecting the resulting catalytic activity can be summarized as follows:

- The incorporation of transition metals into the electrocatalyst design can be advantageous. Although these beneficial effects are tunable, optimal synergistic effects between various metals boost electrocatalytic capabilities.
- The catalyst core/shell design is a realistic and practical strategy to enhance the active sites for HER electrocatalysis while making the material feasible for development. It is particularly effective and successful in increasing active sites around the borders of two-dimensional layered structures. However, although the core/shell design enhances catalytic performance, the overall structure may be inadequate for industrial operation.
- A high-level carbon catalyst is required for support. To obtain adequate performance, even with Pt, a sufficient carbon catalyst support must be utilized (and not just low overpotential). However, the physical and chemical structure of carbon is undeniably important in electrocatalytic efficacy.
- Transition-based chemicals such as sulfides, selenides, phosphides, and carbides are the most promising options.
- The employment of transition metals in electrocatalytic architecture, similar to doping, can be advantageous.

- The substrate surface plays an important role, especially for electroactive monolayers or ultrathin films. This effect is seen on both the smooth surface and the particle coating.
- Planar deformation and strain engineering can assist activate putative electrocatalytic sites on base surfaces.
- MOF-based materials demonstrate significant activity in the HER due to their high porosity, controlled porosity, and suitable structure. These materials are utilized as electrocatalysts for HER for several reasons. First, they offer an opportunity to enhance and replace expensive noble metal-based catalysts with more affordable metals. Second, they aid in reducing the necessary overpotential for HER, thereby improving the overall efficiency. Lastly, MOF-based materials contribute to improved reaction kinetics, enabling more efficient HER processes. Overall, the unique characteristics of MOFs make them promising candidates for HER electrocatalysis.

Despite significant advances in understanding electrocatalytic processes and designing suitable electrodes for the HER, there are several challenges to the cost-effective production of large-scale hydrogen by split water electrolysis. To ensure the successful progress of the research, it is necessary to integrate the test protocol in order to be able to compare different materials. In addition, when designing novel cathodic catalysts in the research phase, the ease of preparation and potential scalability for industrial applications should be considered. However, recent interest in a different approach to energy sources, the importance of environmental protection in the future, and economic issues are expected to lead to new advances in the design of active, sustainable, and low-cost HER electrocatalysts for mass commercialization of water-based hydrogen production.

AUTHOR INFORMATION

Corresponding Authors

Faranak Manteghi – Research Laboratory of Inorganic Chemistry and Environment, Department of Chemistry, Iran University of Science and Technology, 16846-13114 Tehran, Iran; orcid.org/0000-0002-2590-5063; Email: f_manteghi@iust.ac.ir

Zari Tehrani – The Future Manufacturing Research Institute, Faculty of Science and Engineering, Swansea University, SA1 8EN Swansea, United Kingdom; orcid.org/0000-0002-5069-7921; Email: z.tehrani@swansea.ac.uk

Author

Amir Kazemi – Research Laboratory of Inorganic Chemistry and Environment, Department of Chemistry, Iran University of Science and Technology, 16846-13114 Tehran, Iran

Complete contact information is available at:
<https://pubs.acs.org/10.1021/acsomega.3c07911>

Notes

The authors declare no competing financial interest.

ACKNOWLEDGMENTS

The authors gratefully acknowledge the financial support of the Research Council of the Iran University of Science and Technology, Swansea University, and the Royal Academy of Engineering.

REFERENCES

- (1) Shi, Y.; Ma, Z.-R.; Xiao, Y.-Y.; Yin, Y.-C.; Huang, W.-M.; Huang, Z.-C.; Zheng, Y.-Z.; Mu, F.-Y.; Huang, R.; Shi, G.-Y.; et al. Electronic metal-support interaction modulates single-atom platinum catalysis for hydrogen evolution reaction. *Nat. Commun.* **2021**, *12* (1), 1–11.
- (2) Dou, Y.; Wang, A.; Zhao, L.; Yang, X.; Wang, Q.; Sudi, M. S.; Zhu, W.; Shang, D. Boosted hydrogen evolution reaction for a nitrogen-rich azo-bridged metallated porphyrin network. *J. Colloid Interface Sci.* **2023**, *650*, 943–950.
- (3) Vijayapradeep, S.; Logeshwaran, N.; Ramakrishnan, S.; Kim, A. R.; Sampath, P.; Kim, D. H.; Yoo, D. J. Novel Pt-carbon core-shell decorated hierarchical CoMo₂S₄ as efficient electrocatalysts for alkaline/seawater hydrogen evolution reaction. *Chem. Eng. J.* **2023**, *473*, 145348.
- (4) Ramachandran, E.; Krishnaiah, R.; Venkatesan, E. P.; Shaik, S.; Saleel, C. A.; Hussain, F. Investigation into the Ideal Concoction for Performance and Emissions Enhancement of Jatropa Biodiesel-Diesel with CuO Nanoparticles Using Response Surface Methodology. *ACS omega* **2023**, *8* (42), 39067–39079.
- (5) Riaz, A.; Qyyum, M. A.; Hussain, A.; Lee, M. Tapping the energy and exergy benefits of channeling liquid air energy system in the hydrogen liquefaction process. *Journal of Energy Storage* **2023**, *72*, 108193.
- (6) Hoang, A. T.; Pandey, A.; De Osés, F. J. M.; Chen, W.-H.; Said, Z.; Ng, K. H.; Ağbulut, D. C.; Tarelko, W.; Ölçer, A. I.; Nguyen, X. P. Technological solutions for boosting hydrogen role in decarbonization strategies and net-zero goals of world shipping: Challenges and perspectives. *Renewable Sustainable Energy Rev.* **2023**, *188*, 113790.
- (7) Longchamps, R. S.; Yang, X.-G.; Wang, C.-Y. Fundamental Insights into Battery Thermal Management and Safety. *ACS Energy Lett.* **2022**, *7* (3), 1103–1111.
- (8) Li, Y.; Zhou, Q.; Weng, S.; Ding, F.; Qi, X.; Lu, J.; Li, Y.; Zhang, X.; Rong, X.; Lu, Y.; et al. Interfacial engineering to achieve an energy density of over 200 Wh kg⁻¹ in sodium batteries. *Nat. Energy* **2022**, *7* (6), 511–519. Kumar, A.; Bui, V. Q.; Lee, J.; Jadhav, A. R.; Hwang, Y.; Kim, M. G.; Kawazoe, Y.; Lee, H. Modulating interfacial charge density of NiP₂-FeP₂ via coupling with metallic Cu for accelerating alkaline hydrogen evolution. *ACS Energy Lett.* **2021**, *6* (2), 354–363.
- (9) Biggins, F.; Kataria, M.; Roberts, D.; Brown, S. Green hydrogen investments: Investigating the option to wait. *Energy* **2022**, *241*, 122842. Fei, B.; Chen, Z.; Liu, J.; Xu, H.; Yan, X.; Qing, H.; Chen, M.; Wu, R. Ultrathinning nickel sulfide with modulated electron density for efficient water splitting. *Adv. Energy Mater.* **2020**, *10* (41), 2001963.
- (10) Thirumal, V.; Yuvaakumar, R.; Saravanakumar, B.; Ravi, G.; Isacfranklin, M.; Shobana, M.; Al-Sehemi, A. G.; Velauthapillai, D. Carbonization and optimization of biomass waste for HER application. *Fuel* **2022**, *324*, 124466.
- (11) Fakayode, O. A.; Yusuf, B. A.; Zhou, C.; Xu, Y.; Ji, Q.; Xie, J.; Ma, H. Simplistic two-step fabrication of porous carbon-based biomass-derived electrocatalyst for efficient hydrogen evolution reaction. *Energy Conversion and Management* **2021**, *227*, 113628.
- (12) Huner, B.; Demir, N.; Kaya, M. F. Hydrogen Evolution Reaction Performance of Ni-Co-Coated Graphene-Based 3D Printed Electrodes. *ACS omega* **2023**, *8* (6), 5958–5974.
- (13) McCrum, I. T.; Koper, M. The role of adsorbed hydroxide in hydrogen evolution reaction kinetics on modified platinum. *Nature Energy* **2020**, *5* (11), 891–899.
- (14) Hao, J.; Zhuang, Z.; Cao, K.; Gao, G.; Wang, C.; Lai, F.; Lu, S.; Ma, P.; Dong, W.; Liu, T.; et al. Unraveling the electronegativity-dominated intermediate adsorption on high-entropy alloy electrocatalysts. *Nat. Commun.* **2022**, *13* (1), 1–13.
- (15) Tang, Z.; Wei, S.; Wang, Y.; Dai, L. Three-dimensional reduced graphene oxide decorated with cobalt metaphosphate as high cost-efficiency electrocatalysts for the hydrogen evolution reaction. *RSC Adv.* **2022**, *12* (17), 10522–10533.
- (16) Wang, T.; Tao, L.; Zhu, X.; Chen, C.; Chen, W.; Du, S.; Zhou, Y.; Zhou, B.; Wang, D.; Xie, C.; et al. Combined anodic and cathodic hydrogen production from aldehyde oxidation and hydrogen evolution reaction. *Nat. Catal.* **2022**, *5* (1), 66–73.
- (17) Song, D.; Sun, J.; Sun, L.; Zhai, S.; Ho, G. W.; Wu, H.; Deng, W. Q. Acidic media regulated hierarchical cobalt compounds with phosphorous doping as water splitting electrocatalysts. *Adv. Energy Mater.* **2021**, *11* (22), 2100358.
- (18) Voitic, G.; Hacker, V. Recent advancements in chemical looping water splitting for the production of hydrogen. *Rsc Advances* **2016**, *6* (100), 98267–98296.
- (19) Hermesmann, M.; Müller, T. Green, Turquoise, Blue, or Grey? Environmentally friendly Hydrogen Production in Transforming Energy Systems. *Prog. Energy Combust. Sci.* **2022**, *90*, 100996. Haverkort, J.; Rajaei, H. Voltage losses in zero-gap alkaline water electrolysis. *J. Power Sources* **2021**, *497*, 229864.
- (20) Li, Y.; Shi, X.; Phoumin, H. A strategic roadmap for large-scale green hydrogen demonstration and commercialisation in China: A review and survey analysis. *Int. J. Hydrogen Energy* **2022**, *47*, 24592–24609.
- (21) Miller, H. A.; Bouzek, K.; Hnat, J.; Loos, S.; Bernäcker, C. I.; Weißgärber, T.; Röntzsch, L.; Meier-Haack, J. Green hydrogen from anion exchange membrane water electrolysis: a review of recent developments in critical materials and operating conditions. *Sustainable Energy & Fuels* **2020**, *4* (5), 2114–2133.
- (22) Zhang, P.; Cheng, H.; Gu, F.; Hong, S.; Dong, H.; Li, C. Progress on iron-series metal-organic frameworks materials towards electrocatalytic hydrogen evolution reaction. *Surfaces and Interfaces* **2023**, *42*, 103368.
- (23) Wang, J.; Gao, Y.; Kong, H.; Kim, J.; Choi, S.; Ciucci, F.; Hao, Y.; Yang, S.; Shao, Z.; Lim, J. Non-precious-metal catalysts for alkaline water electrolysis: operando characterizations, theoretical calculations, and recent advances. *Chem. Soc. Rev.* **2020**, *49* (24), 9154–9196.
- (24) Dinh, K. N.; Sun, Y.; Pei, Z.; Yuan, Z.; Suwardi, A.; Huang, Q.; Liao, X.; Wang, Z.; Chen, Y.; Yan, Q. Electronic modulation of nickel disulfide toward efficient water electrolysis. *Small* **2020**, *16* (17), 1905885. Grigoriev, S.; Fateev, V.; Bessarabov, D.; Millet, P. Current status, research trends, and challenges in water electrolysis science and technology. *Int. J. Hydrogen Energy* **2020**, *45* (49), 26036–26058.
- (25) Wan, L.; Xu, Z.; Wang, P.; Lin, Y.; Wang, B. H₂SO₄-doped polybenzimidazole membranes for hydrogen production with acid-alkaline amphoteric water electrolysis. *J. Membr. Sci.* **2021**, *618*, 118642. Cheikh, J. A.; Zakari, R.; Bhosale, A. C.; Villagra, A.; Leclerc, N.; Floquet, S.; Ghosh, P. C.; Ranjbari, A.; Cadot, E.; Millet, P.; et al. Electrocatalytic properties of {Mo₃S₄}⁻-based complexes with regard to the hydrogen evolution reaction and application to PEM water electrolysis. *Mater. Adv.* **2020**, *1* (3), 430–440.
- (26) Huang, W.-H.; Li, X.-M.; Yang, X.-F.; Zhang, H.-B.; Wang, F.; Zhang, J. Highly efficient electrocatalysts for overall water splitting: mesoporous CoS/MoS₂ with hetero-interfaces. *Chem. Commun.* **2021**, *57* (39), 4847–4850. Ji, Y.; Liu, J.; Hao, S.; Xiao, Y.; Li, L.; Liu, X. Full water splitting by a nanoporous CeO₂ nanowire array under alkaline conditions. *Inorganic Chemistry Frontiers* **2020**, *7* (13), 2533–2537.
- (27) Lin, L.; Sherrell, P.; Liu, Y.; Lei, W.; Zhang, S.; Zhang, H.; Wallace, G. G.; Chen, J. Engineered 2D transition metal dichalcogenides—a vision of viable hydrogen evolution reaction catalysis. *Adv. Energy Mater.* **2020**, *10* (16), 1903870.
- (28) Wang, X.; Zheng, Y.; Sheng, W.; Xu, Z. J.; Jaroniec, M.; Qiao, S.-Z. Strategies for design of electrocatalysts for hydrogen evolution under alkaline conditions. *Mater. Today* **2020**, *36*, 125–138. Pu, Z.; Amiin, I. S.; Cheng, R.; Wang, P.; Zhang, C.; Mu, S.; Zhao, W.; Su, F.; Zhang, G.; Liao, S.; et al. Single-atom catalysts for electrochemical hydrogen evolution reaction: recent advances and future perspectives. *Nano-Micro Lett.* **2020**, *12* (1), 1–29. Shang, P.; Ye, Z.; Ding, Y.; Zhu, Z.; Peng, X.; Ma, G.; Li, D. Nanosponge-like solid solution of NiMo with a high hydrogen evolution reaction performance over a wide range of current densities. *ACS Sustainable Chem. Eng.* **2020**, *8* (29), 10664–10672.
- (29) Liu, Y.; Yong, X.; Liu, Z.; Chen, Z.; Kang, Z.; Lu, S. Unified catalyst for efficient and stable hydrogen production by both the electrolysis of water and the hydrolysis of ammonia borane. *Adv. Sustainable Syst.* **2019**, *3* (5), 1800161. dos Santos, K. G.; Eckert, C. T.; De Rossi, E.; Baricatti, R. A.; Frigo, E. P.; Lindino, C. A.; Alves, H. J.

Hydrogen production in the electrolysis of water in Brazil, a review. *Renewable and Sustainable Energy Reviews* **2017**, *68*, 563–571.

(30) Wang, Y.; Sun, D.; Wang, M.; Feng, Z.; Hall, A. S. Oxygen Reduction Electrocatalysis on Ordered Intermetallic Pd-Bi Electrodes Is Enhanced by a Low Coverage of Spectator Species. *J. Phys. Chem. C* **2020**, *124* (9), 5220–5224. Wang, J.; Qiu, T.; Chen, X.; Lu, Y.; Yang, W. N-doped carbon@ Ni-Al₂O₃ nanosheet array@ graphene oxide composite as an electrocatalyst for hydrogen evolution reaction in alkaline medium. *J. Power Sources* **2015**, *293*, 178–186. Schmidt, T. J.; Stamenkovic, V.; Ross, P. N., Jr.; Markovic, N. M. Temperature dependent surface electrochemistry on Pt single crystals in alkaline electrolyte Part 3. The oxygen reduction reaction. *Phys. Chem. Chem. Phys.* **2003**, *5* (2), 400–406.

(31) Cai, J.; Ding, J.; Wei, D.; Xie, X.; Li, B.; Lu, S.; Zhang, J.; Liu, Y.; Cai, Q.; Zang, S. Coupling of Ru and O-Vacancy on 2D Mo-Based Electrocatalyst Via a Solid-Phase Interface Reaction Strategy for Hydrogen Evolution Reaction. *Adv. Energy Mater.* **2021**, *11* (26), 2100141. Kou, T.; Chen, M.; Wu, F.; Smart, T. J.; Wang, S.; Wu, Y.; Zhang, Y.; Li, S.; Lall, S.; Zhang, Z. J. N. c.; et al. Carbon doping switching on the hydrogen adsorption activity of NiO for hydrogen evolution reaction. *Nat. Commun.* **2020**, *11* (1), 1–10. Li, W.; Liu, G.; Li, J.; Wang, Y.; Ricardez-Sandoval, L.; Zhang, Y.; Zhang, Z. J. A. S. S. Hydrogen evolution reaction mechanism on 2H-MoS₂ electrocatalyst. *Appl. Surf. Sci.* **2019**, *498*, 143869. Liu, Z.; Yang, X.; Hu, G.; Feng, L. Ru nanoclusters coupled on Co/N-doped carbon nanotubes efficiently catalyzed the hydrogen evolution reaction. *ACS Sustainable Chem. Eng.* **2020**, *8* (24), 9136–9144. Zhou, M.; Li, H.; Long, A.; Zhou, B.; Lu, F.; Zhang, F.; Zhan, F.; Zhang, Z.; Xie, W.; Zeng, X.; et al. Modulating 3d Orbitals of Ni Atoms on Ni-Pt Edge Sites Enables Highly-Efficient Alkaline Hydrogen Evolution. *Adv. Energy Mater.* **2021**, *11* (36), 2101789.

(32) Yu, X.; Xu, S.; Wang, Z.; Cheng, X.; Du, Y.; Chen, G.; Sun, X.; Wu, Q. An Mn-doped NiCoP flower-like structure as a highly efficient electrocatalyst for hydrogen evolution reaction in acidic and alkaline solutions with long duration. *Nanoscale* **2021**, *13* (25), 11069–11076.

(33) He, H.-z.; Zhang, Y.; Li, Y.; Wang, P. Recent innovations of silk-derived electrocatalysts for hydrogen evolution reaction, oxygen evolution reaction and oxygen reduction reaction. *Int. J. Hydrogen Energy* **2021**, *46* (11), 7848–7865.

(34) Wen, Q.; Zhao, Y.; Liu, Y.; Li, H.; Zhai, T. Ultrahigh-Current-Density and Long-Term-Durability Electrocatalysts for Water Splitting. *Small* **2022**, *18* (4), 2104513. Hao, J.; Wei, F.; Zhang, X.; Li, L.; Zhang, C.; Liang, D.; Ma, X.; Lu, P. Defect and doping engineered pentagraphene for catalysis of hydrogen evolution reaction. *Nanoscale Res. Lett.* **2021**, *16* (1), 1–9.

(35) Wang, S.; Xu, B.; Huo, W.; Feng, H.; Zhou, X.; Fang, F.; Xie, Z.; Shang, J. K.; Jiang, J. Efficient FeCoNiCuPd thin-film electrocatalyst for alkaline oxygen and hydrogen evolution reactions. *Appl. Catal. B: Environmental* **2022**, *313*, 121472.

(36) Tymoczko, J.; Calle-Vallejo, F.; Schuhmann, W.; Bandarenka, A. S. Making the hydrogen evolution reaction in polymer electrolyte membrane electrolyzers even faster. *Nat. Commun.* **2016**, *7* (1), 1–6. Lačnjevac, U.; Vasilic, R.; Dobrota, A.; Đurđić, S.; Tomanec, O.; Zbořil, R.; Mohajernia, S.; Nguyen, N. T.; Skorodumova, N.; Manojlović, D.; et al. High-performance hydrogen evolution electrocatalysis using proton-intercalated TiO₂ nanotube arrays as interactive supports for Ir nanoparticles. *J. Mater. Chem. A* **2020**, *8* (43), 22773–22790. Zhang, W.; Huang, B.; Wang, K.; Yang, W.; Lv, F.; Li, N.; Chao, Y.; Zhou, P.; Yang, Y.; Li, Y.; et al. WO_x-Surface Decorated PtNi@ Pt Dendritic Nanowires as Efficient pH-Universal Hydrogen Evolution Electrocatalysts. *Adv. Energy Mater.* **2021**, *11* (3), 2003192.

(37) Wendt, H.; Spinacé, E. V.; Oliveira Neto, A.; Linardi, M. J. Q. N. Electrocatalysis and electrocatalysts for low temperature fuel cells: fundamentals, state of the art, research and development. *Química Nova* **2005**, *28* (6), 1066–1075. Koper, M. T. Thermodynamic theory of multi-electron transfer reactions: Implications for electrocatalysis. *J. Electroanal. Chem.* **2011**, *660* (2), 254–260.

(38) Sheng, W.; Myint, M.; Chen, J. G.; Yan, Y. J. E. Correlating the hydrogen evolution reaction activity in alkaline electrolytes with the

hydrogen binding energy on monometallic surfaces. *Energy Environ. Sci.* **2013**, *6* (5), 1509–1512.

(39) Zheng, Y.; Jiao, Y.; Vasileff, A.; Qiao, S. Z. The hydrogen evolution reaction in alkaline solution: from theory, single crystal models, to practical electrocatalysts. *Angew. Chem., Int. Ed.* **2018**, *57* (26), 7568–7579.

(40) Kim, J.; Jung, H.; Jung, S.-M.; Hwang, J.; Kim, D. Y.; Lee, N.; Kim, K.-S.; Kwon, H.; Kim, Y.-T.; Han, J. W.; et al. Tailoring binding abilities by incorporating oxophilic transition metals on 3D nanostructured Ni arrays for accelerated alkaline hydrogen evolution reaction. *J. Am. Chem. Soc.* **2021**, *143* (3), 1399–1408. Ugwu, L. I.; Morgan, Y.; Ibrahim, H. Application of density functional theory and machine learning in heterogenous-based catalytic reactions for hydrogen production. *Int. J. Hydrogen Energy* **2022**, *47* (4), 2245–2267.

(41) Ibn Shamsah, S. M. Earth-abundant electrocatalysts for water splitting: current and future directions. *Catalysts* **2021**, *11* (4), 429.

(42) Krishtalik, L. I. Kinetic isotope effect in the hydrogen evolution reaction. *Electrochimica Acta* **2001**, *46* (19), 2949–2960. Qi, Q.; Shao, D.; Zhou, Y.; Wang, Q.; Yu, X.-Y. Plasma-induced implanting of active species in metal-organic frameworks for efficient hydrogen evolution reaction. *Journal of Materials Chemistry A* **2023**, *11* (29), 15663–15669.

(43) Wu, H.; Feng, C.; Zhang, L.; Zhang, J.; Wilkinson, D. P. Non-noble metal electrocatalysts for the hydrogen evolution reaction in water electrolysis. *Electrochemical Energy Reviews* **2021**, *4* (3), 473–507.

(44) Zhou, F.; Zhou, Y.; Liu, G.-G.; Wang, C.-T.; Wang, J. Recent advances in nanostructured electrocatalysts for hydrogen evolution reaction. *Rare Metals* **2021**, *40* (12), 3375–3405. Chen, L.-W.; Liang, H.-W. Ir-based bifunctional electrocatalysts for overall water splitting. *Catal. Sci. Technol.* **2021**, *11*, 4673–4689.

(45) Zhang, X.-Y.; Xie, J.-Y.; Ma, Y.; Dong, B.; Liu, C.-G.; Chai, Y.-M. An overview of the active sites in transition metal electrocatalysts and their practical activity for hydrogen evolution reaction. *Chem. Eng. J.* **2022**, *430*, 132312.

(46) Theerthagiri, J.; Lee, S. J.; Murthy, A. P.; Madhavan, J.; Choi, M. Y. Fundamental aspects and recent advances in transition metal nitrides as electrocatalysts for hydrogen evolution reaction: A review. *Curr. Opin. Solid State Mater. Sci.* **2020**, *24* (1), 100805.

(47) Ge, Z.; Fu, B.; Zhao, J.; Li, X.; Ma, B.; Chen, Y. A review of the electrocatalysts on hydrogen evolution reaction with an emphasis on Fe, Co and Ni-based phosphides. *J. Mater. Sci.* **2020**, *55* (29), 14081–14104.

(48) Anantharaj, S.; Kundu, S.; Noda, S. Progress in nickel chalcogenide electrocatalyzed hydrogen evolution reaction. *Journal of Materials Chemistry A* **2020**, *8* (8), 4174–4192.

(49) Li, T.; Hu, T.; Dai, L.; Li, C. M. Metal-free photo-and electrocatalysts for hydrogen evolution reaction. *Journal of Materials Chemistry A* **2020**, *8* (45), 23674–23698.

(50) Luo, W.; Wang, Y.; Cheng, C. Ru-based electrocatalysts for hydrogen evolution reaction: recent research advances and perspectives. *Materials Today Physics* **2020**, *15*, 100274. Ogundipe, T. O.; Shen, L.; Lu, Z.; Yan, C.; Yan, C. Recent Advances on Bimetallic Transition Metal Phosphides for Enhanced Hydrogen Evolution Reaction. *ChemistrySelect* **2022**, *7* (23), No. e202200291.

(51) Chen, Q.; Yu, Y.; Li, J.; Nan, H.; Luo, S.; Jia, C.; Deng, P.; Zhong, S.; Tian, X. Recent Progress in Layered Double Hydroxide-Based Electrocatalyst for Hydrogen Evolution Reaction. *ChemElectroChem* **2022**, *9* (9), No. e202101387. Zhou, D.; Li, P.; Lin, X.; McKinley, A.; Kuang, Y.; Liu, W.; Lin, W.-F.; Sun, X.; Duan, X. Layered double hydroxide-based electrocatalysts for the oxygen evolution reaction: identification and tailoring of active sites, and superaerophobic nanoarray electrode assembly. *Chem. Soc. Rev.* **2021**, *50* (15), 8790–8817.

(52) Chen, J.; Cheng, H.; Ding, L.-X.; Wang, H. Competing hydrogen evolution reaction: a challenge in electrocatalytic nitrogen fixation. *Materials Chemistry Frontiers* **2021**, *5* (16), 5954–5969. Zhu, J.; Yang, R.; Zhang, G. Atomically thin transition metal dichalcogenides for the hydrogen evolution reaction. *ChemPhysMater.* **2022**, *1*, 102.

(53) Hansen, J. N.; Prats, H.; Toudahl, K. K.; Mørch Secher, N.; Chan, K.; Kibsgaard, J.; Chorkendorff, I. Is there anything better than Pt for

- HER? *ACS energy letters* **2021**, *6* (4), 1175–1180. Beyene, B. B.; Hung, C.-H. Recent progress on metalloporphyrin-based hydrogen evolution catalysis. *Coord. Chem. Rev.* **2020**, *410*, 213234.
- (54) Aggarwal, P.; Sarkar, D.; Awasthi, K.; Menezes, P. W. Functional role of single-atom catalysts in electrocatalytic hydrogen evolution: Current developments and future challenges. *Coord. Chem. Rev.* **2022**, *452*, 214289.
- (55) Zahra, R.; Pervaiz, E.; Yang, M.; Rabi, O.; Saleem, Z.; Ali, M.; Farrukh, S. A review on nickel cobalt sulphide and their hybrids: Earth abundant, pH stable electro-catalyst for hydrogen evolution reaction. *Int. J. Hydrogen Energy* **2020**, *45* (46), 24518–24543.
- (56) Yang, W.; Chen, S. Recent progress in electrode fabrication for electrocatalytic hydrogen evolution reaction: A mini review. *Chem. Eng. J.* **2020**, *393*, 124726.
- (57) Chen, S.; Pan, Y. Influence of group III and IV elements on the hydrogen evolution reaction of MoS₂ disulfide. *J. Phys. Chem. C* **2021**, *125* (22), 11848–11856.
- (58) Feng, W.; Pang, W.; Xu, Y.; Guo, A.; Gao, X.; Qiu, X.; Chen, W. Transition metal selenides for electrocatalytic hydrogen evolution reaction. *ChemElectroChem* **2020**, *7* (1), 31–54.
- (59) Drosou, M.; Kamatsos, F.; Mitsopoulou, C. A. Recent advances in the mechanisms of the hydrogen evolution reaction by non-innocent sulfur-coordinating metal complexes. *Inorganic Chemistry Frontiers* **2020**, *7* (1), 37–71.
- (60) Liu, Y.; Wang, Q.; Zhang, J.; Ding, J.; Cheng, Y.; Wang, T.; Li, J.; Hu, F.; Yang, H. B.; Liu, B. Recent Advances in Carbon-Supported Noble-Metal Electrocatalysts for Hydrogen Evolution Reaction: Syntheses, Structures, and Properties. *Adv. Energy Mater.* **2022**, *12*, 2200928.
- (61) Zheng, X.; Peng, L.; Li, L.; Yang, N.; Yang, Y.; Li, J.; Wang, J.; Wei, Z. J. C. s. Role of non-metallic atoms in enhancing the catalytic activity of nickel-based compounds for hydrogen evolution reaction. *Chemical science* **2018**, *9* (7), 1822–1830.
- (62) Kozhushner, A.; Zion, N.; Elbaz, L. J. C. O. i. E. Methods for assessment and measurement of the active site density in platinum group metal-free oxygen reduction reaction catalysts. *Current Opinion in Electrochemistry* **2021**, *25*, 100620. Carmo, M.; Fritz, D. L.; Mergel, J.; Stolten, D. A comprehensive review on PEM water electrolysis. *Int. J. Hydrogen Energy* **2013**, *38* (12), 4901–4934. Safizadeh, F.; Ghali, E.; Houlachi, G. Electrocatalysis developments for hydrogen evolution reaction in alkaline solutions-A review. *Int. J. Hydrogen Energy* **2015**, *40* (1), 256–274.
- (63) Markovića, N. M.; Sarraf, S. T.; Gasteiger, H. A.; Ross, P. N. Faraday Transactions. Hydrogen electrochemistry on platinum low-index single-crystal surfaces in alkaline solution. *J. Chem. Soc., Faraday Trans.* **1996**, *92* (20), 3719–3725. Gottesfeld, S. *Fuel cell science: Theory, fundamentals, and biocatalysis*; John Wiley & Sons: New York, 2011. Kobayashi, S.; Tryk, D.; Uchida, H. J. E. C. Enhancement of hydrogen evolution activity on Pt-skin/Pt₃Co [(111),(100), and (110)] single crystal electrodes. *Electrochem. Commun.* **2020**, *110*, 106615.
- (64) Lee, W.-J.; Wan, Z.; Kim, C.-M.; Oh, I.-K.; Harada, R.; Suzuki, K.; Choi, E.-A.; Kwon, S.-H. J. C. o. M. Atomic layer deposition of Pt thin films using dimethyl (N, N-dimethyl-3-butene-1-amine-N) platinum and O₂ reactant. *Chem. Mater.* **2019**, *31* (14), 5056–5064. Lopes, P. P.; Li, D.; Lv, H.; Wang, C.; Tripkovic, D.; Zhu, Y.; Schimmenti, R.; Daimon, H.; Kang, Y.; Snyder, J. J. N. M.; et al. Eliminating dissolution of platinum-based electrocatalysts at the atomic scale. *Nat. Mater.* **2020**, *19* (11), 1207–1214.
- (65) Fu, H. Q.; Zhou, M.; Liu, P. F.; Liu, P.; Yin, H.; Sun, K. Z.; Yang, H. G.; Al-Mamun, M.; Hu, P.; Wang, H.-F.; et al. Hydrogen spillover-bridged Volmer/Tafel processes enabling ampere-level current density alkaline hydrogen evolution reaction under low overpotential. *J. Am. Chem. Soc.* **2022**, *144* (13), 6028–6039. Lao, M.; Li, P.; Jiang, Y.; Pan, H.; Dou, S. X.; Sun, W. From Fundamentals and Theories to Heterostructured Electrocatalyst Design: An In-depth Understanding of Alkaline Hydrogen Evolution Reaction. *Nano Energy* **2022**, *98*, 107231.
- (66) Zhai, L.; She, X.; Zhuang, L.; Li, Y.; Ding, R.; Guo, X.; Zhang, Y.; Zhu, Y.; Xu, K.; Fan, H. J.; et al. Modulating Built-In Electric Field via Variable Oxygen Affinity for Robust Hydrogen Evolution Reaction in Neutral Media. *Angew. Chem., Int. Ed.* **2022**, *61* (14), No. e202116057. Chen, Y.; Ding, R.; Li, J.; Liu, J. Highly active atomically dispersed platinum-based electrocatalyst for hydrogen evolution reaction achieved by defect anchoring strategy. *Appl. Catal. B: Environmental* **2022**, *301*, 120830.
- (67) Ghamami, S.; Kazemi Korayem, A.; Baqeri, N. Production and purification of titanium dioxide with titanium tetrachloride nanoparticles from eliminate concentrate of Kahnooj mine in Kerman. *J. Appl. Chem.* **2020**, *15* (55), 189–206. Ren, B.; Jin, Q.; Li, Y.; Li, Y.; Cui, H.; Wang, C. Activating titanium dioxide as a new efficient electrocatalyst: from theory to experiment. *ACS Appl. Mater. Interfaces* **2020**, *12* (10), 11607–11615.
- (68) Kweon, D. H.; Okyay, M. S.; Kim, S.-J.; Jeon, J.-P.; Noh, H.-J.; Park, N.; Mahmood, J.; Baek, J.-B. Ruthenium anchored on carbon nanotube electrocatalyst for hydrogen production with enhanced Faradaic efficiency. *Nat. Commun.* **2020**, *11* (1), 1–10.
- (69) Bao, X.; Chen, Y.; Mao, S.; Wang, Y.; Yang, Y.; Gong, Y. Boosting the performance gain of Ru/C for hydrogen evolution reaction via surface engineering. *Energy Environ. Mater.* **2023**, *6* (5).
- (70) Malik, B.; Anantharaj, S.; Karthick, K.; Pattanayak, D. K.; Kundu, S. J. C. S. Technology. Magnetic CoPt nanoparticle-decorated ultrathin Co (OH)₂ nanosheets: an efficient bi-functional water splitting catalyst. *Catalysis Science & Technology* **2017**, *7* (12), 2486–2497. Thiel, F.; Geissler, D.; Nielsch, K.; Kauffmann, A.; Seils, S.; Heilmaier, M.; Utt, D.; Albe, K.; Motylenko, M.; Rafaja, D. J. A. M.; et al. Origins of strength and plasticity in the precious metal based high-entropy alloy AuCuNiPdPt. *Acta Mater.* **2020**, *185*, 400–411. Liu, H.; Xi, C.; Xin, J.; Zhang, G.; Zhang, S.; Zhang, Z.; Huang, Q.; Li, J.; Liu, H.; Kang, J. J. C. E. J. Free-standing nanoporous NiMnFeMo alloy: An efficient non-precious metal electrocatalyst for water splitting. *Chem. Eng. J.* **2021**, *404*, 126530.
- (71) Scofield, M. E.; Zhou, Y.; Yue, S.; Wang, L.; Su, D.; Tong, X.; Vukmirovic, M. B.; Adzic, R. R.; Wong, S. S. Role of chemical composition in the enhanced catalytic activity of Pt-based alloyed ultrathin nanowires for the hydrogen oxidation reaction under alkaline conditions. *ACS Catal.* **2016**, *6* (6), 3895–3908.
- (72) Santos, D.; Sequeira, C.; Macciò, D.; Saccone, A.; Figueiredo, J. Platinum-rare earth electrodes for hydrogen evolution in alkaline water electrolysis. *International journal of hydrogen energy* **2013**, *38* (8), 3137–3145. Stojić, D. L.; Grozdić, T. D.; Kaninski, M. M.; Maksić, A. D.; Simić, N. D. Intermetallics as advanced cathode materials in hydrogen production via electrolysis. *International journal of hydrogen energy* **2006**, *31* (7), 841–846.
- (73) Naveen, M. H.; Huang, Y.; Bisalere Kantharajappa, S.; Seo, K.-D.; Park, D.-S.; Shim, Y.-B. Enhanced electrocatalytic activities of in situ produced Pd/S/N-doped carbon in oxygen reduction and hydrogen evolution reactions. *ACS Appl. Energy Mater.* **2021**, *4* (1), 575–585.
- (74) Zhang, L.; Xiao, W.; Zhang, Y.; Han, F.; Yang, X. Nanocarbon encapsulating Ni-doped MoP/graphene composites for highly improved electrocatalytic hydrogen evolution reaction. *Compos. Commun.* **2021**, *26*, 100792.
- (75) Pu, M.; Wang, D.; Zhang, Z.; Guo, Y.; Guo, W. Flexoelectricity enhanced water splitting and hydrogen evolution reaction on grain boundaries of monolayer transition metal dichalcogenides. *Nano Research* **2022**, *15* (2), 978–984.
- (76) Lai, J.; Huang, B.; Chao, Y.; Chen, X.; Guo, S. J. A. M. Strongly Coupled Nickel-Cobalt Nitrides/Carbon Hybrid Nanocages with Pt-Like Activity for Hydrogen Evolution Catalysis. *Adv. Mater.* **2019**, *31* (2), 1805541.
- (77) Kuttiyiel, K. A.; Sasaki, K.; Chen, W.-F.; Su, D.; Adzic, R. R. Core-shell, hollow-structured iridium-nickel nitride nanoparticles for the hydrogen evolution reaction. *J. Mater. Chem. A* **2014**, *2* (3), 591–594.
- (78) Zhang, L.; Wang, T.; Sun, L.; Sun, Y.; Hu, T.; Xu, K.; Ma, F. Hydrothermal synthesis of 3D hierarchical MoSe₂/NiSe₂ composite nanowires on carbon fiber paper and their enhanced electrocatalytic

- activity for the hydrogen evolution reaction. *J. Mater. Chem. A* **2017**, *5* (37), 19752–19759.
- (79) Wang, X.; Zheng, Y.; Yuan, J.; Shen, J.; Hu, J.; Wang, A.-j.; Wu, L.; Niu, L. J. E. A. Porous NiCo diselenide nanosheets arrayed on carbon cloth as promising advanced catalysts used in water splitting. *Electrochim. Acta* **2017**, *225*, 503–513.
- (80) Chen, Q.; Wang, R.; Yu, M.; Zeng, Y.; Lu, F.; Kuang, X.; Lu, X. J. E. A. Bifunctional iron-nickel nitride nanoparticles as flexible and robust electrode for overall water splitting. *Electrochim. Acta* **2017**, *247*, 666–673.
- (81) Chen, Y.; Zhang, J.; Guo, P.; Liu, H.; Wang, Z.; Liu, M.; Zhang, T.; Wang, S.; Zhou, Y.; Lu, X. J. A. a. m.; et al. interfaces. Coupled heterostructure of Mo-Fe selenide nanosheets supported on carbon paper as an integrated electrocatalyst for efficient hydrogen evolution. *ACS Appl. Mater.* **2018**, *10* (33), 27787–27794.
- (82) Zhang, N.; Cao, L.; Feng, L.; Huang, J.; Kajiyoshi, K.; Li, C.; Liu, Q.; Yang, D.; He, J. J. N. Co, N-Codoped porous vanadium nitride nanoplates as superior bifunctional electrocatalysts for hydrogen evolution and oxygen reduction reactions. *Nanoscale* **2019**, *11* (24), 11542–11549.
- (83) Read, C. G.; Callejas, J. F.; Holder, C. F.; Schaak, R. E. J. A. a. m. interfaces. General strategy for the synthesis of transition metal phosphide films for electrocatalytic hydrogen and oxygen evolution. *ACS applied materials* **2016**, *8* (20), 12798–12803.
- (84) Pan, Y.; Lin, Y.; Chen, Y.; Liu, Y.; Liu, C. Cobalt phosphide-based electrocatalysts: synthesis and phase catalytic activity comparison for hydrogen evolution. *J. Mater. Chem. A* **2016**, *4* (13), 4745–4754.
- (85) Wang, M.-Q.; Tang, C.; Ye, C.; Duan, J.; Li, C.; Chen, Y.; Bao, S.-J.; Xu, M. J. J. o. M. C. A. Engineering the nanostructure of molybdenum nitride nanodot embedded N-doped porous hollow carbon nanochains for rapid all pH hydrogen evolution. *J. Mater. Chem. A* **2018**, *6* (30), 14734–14741.
- (86) Callejas, J. F.; McEnaney, J. M.; Read, C. G.; Crompton, J. C.; Biacchi, A. J.; Popczun, E. J.; Gordon, T. R.; Lewis, N. S.; Schaak, R. E. J. A. n. Electrocatalytic and photocatalytic hydrogen production from acidic and neutral-pH aqueous solutions using iron phosphide nanoparticles. *ACS Nano* **2014**, *8* (11), 11101–11107.
- (87) Liu, Y.; Kelly, T. G.; Chen, J. G.; Mustain, W. E. J. A. C. Metal carbides as alternative electrocatalyst supports. *ACS Catal.* **2013**, *3* (6), 1184–1194.
- (88) Ramesh, R.; Nandi, D. K.; Kim, T. H.; Cheon, T.; Oh, J.; Kim, S.-H. J. A. a. m. xsinterfaces. Atomic-layer-deposited MoN x thin films on three-dimensional Ni foam as efficient catalysts for the electrochemical hydrogen evolution reaction. *ACS applied materials* **2019**, *11* (19), 17321–17332.
- (89) Zhou, Y.; Yang, Y.; Wang, R.; Wang, X.; Zhang, X.; Qiang, L.; Wang, W.; Wang, Q.; Hu, Z. Rhombic porous CoP 2 nanowire arrays synthesized by alkaline etching as highly active hydrogen-evolution-reaction electrocatalysts. *J. Mater. Chem. A* **2018**, *6* (39), 19038–19046.
- (90) Jin, H.; Liu, X.; Vasileff, A.; Jiao, Y.; Zhao, Y.; Zheng, Y.; Qiao, S.-Z. J. A. N. Single-crystal nitrogen-rich two-dimensional Mo5N6 nanosheets for efficient and stable seawater splitting. *ACS Nano* **2018**, *12* (12), 12761–12769.
- (91) Yu, M.; Zhao, S.; Feng, H.; Hu, L.; Zhang, X.; Zeng, Y.; Tong, Y.; Lu, X. J. A. E. L. Engineering thin MoS2 nanosheets on TiN nanorods: advanced electrochemical capacitor electrode and hydrogen evolution electrocatalyst. *ACS Energy Lett.* **2017**, *2* (8), 1862–1868.
- (92) Chen, T.; Tan, Y. J. N. R. Hierarchical CoNiSe2 nano-architecture as a high-performance electrocatalyst for water splitting. *Nano Research* **2018**, *11* (3), 1331–1344.
- (93) Jiao, C.; Bo, X.; Zhou, M. J. J. o. E. C. Electrocatalytic water splitting at nitrogen-doped carbon layers-encapsulated nickel cobalt selenide. *J. Energy Chem.* **2019**, *34*, 161–170.
- (94) Liang, C.; Ying, P.; Li, C. J. C. o. m. Nanostructured β -Mo2C prepared by carbothermal hydrogen reduction on ultrahigh surface area carbon material. *Chemistry of materials* **2002**, *14* (7), 3148–3151.
- (95) Shi, Z.; Wang, Y.; Lin, H.; Zhang, H.; Shen, M.; Xie, S.; Zhang, Y.; Gao, Q.; Tang, Y. Porous nanoMoC@ graphite shell derived from a MOFs-directed strategy: an efficient electrocatalyst for the hydrogen evolution reaction. *J. Mater. Chem. A* **2016**, *4* (16), 6006–6013.
- (96) Cao, B.; Veith, G. M.; Neufeind, J. C.; Adzic, R. R.; Khalifah, P. G. Mixed close-packed cobalt molybdenum nitrides as non-noble metal electrocatalysts for the hydrogen evolution reaction. *J. Am. Chem. Soc.* **2013**, *135* (51), 19186–19192.
- (97) Chen, W. F.; Schneider, J. M.; Sasaki, K.; Wang, C. H.; Schneider, J.; Iyer, S.; Iyer, S.; Zhu, Y.; Muckerman, J. T.; Fujita, E. J. C. Tungsten carbide-nitride on graphene nanoplatelets as a durable hydrogen evolution electrocatalyst. *ChemSusChem* **2014**, *7* (9), 2414–2418.
- (98) Fang, Z.; Peng, L.; Qian, Y.; Zhang, X.; Xie, Y.; Cha, J. J.; Yu, G. Dual tuning of Ni-Co-A (A= P, Se, O) nanosheets by anion substitution and hole engineering for efficient hydrogen evolution. *J. Am. Chem. Soc.* **2018**, *140* (15), 5241–5247.
- (99) Wang, J.; Yang, W.; Liu, J. CoP 2 nanoparticles on reduced graphene oxide sheets as a super-efficient bifunctional electrocatalyst for full water splitting. *J. Mater. Chem. A* **2016**, *4* (13), 4686–4690.
- (100) Majhi, K. C.; Yadav, M. Fuels. Sphere-Shaped Bimetallic Sulphoselenide: An Efficient Electrocatalyst for Hydrogen Evolution Reaction. *Energy* **2021**, *35* (15), 12473–12481. Li, D.; Liao, L.; Zhou, H.; Zhao, Y.; Cai, F.; Zeng, J.; Liu, F.; Wu, H.; Tang, D.; Yu, F. J. M. T. P. Highly active non-noble electrocatalyst from Co2P/Ni2P nano-hybrids for pH-universal hydrogen evolution reaction. *Materials Today Physics* **2021**, *16*, 100314. Hua, W.; Sun, H.-H.; Xu, F.; Wang, J.-G. J. R. M. A review and perspective on molybdenum-based electrocatalysts for hydrogen evolution reaction. *Rare Metals* **2020**, *39* (4), 335–351. Zhang, W.; Cui, L.; Liu, J. J. J. o. A. Compounds. Recent advances in cobalt-based electrocatalysts for hydrogen and oxygen evolution reactions. *Journal of Alloys* **2020**, *821*, 153542.
- (101) Lin, F.; Dong, Z.; Yao, Y.; Yang, L.; Fang, F.; Jiao, L. Electrocatalytic hydrogen evolution of ultrathin Co-Mo5N6 hetero-junction with interfacial electron redistribution. *Adv. Energy Mater.* **2020**, *10* (42), 2002176.
- (102) Zhang, F.; Shan, W.; Hu, Q.; Jiang, W.; Li, D.; Zhang, B. The Effect of Mo Addition on Electrocatalytic Activity and Stability of Fe-Co-PC Metallic Glasses for Hydrogen Evolution. *J. Electrochem. Soc.* **2021**, *168* (7), 076510. Pentland, N.; Bockris, J. M.; Sheldon, E. Hydrogen evolution reaction on copper, gold, molybdenum, palladium, rhodium, and iron: mechanism and measurement technique under high purity conditions. *J. Electrochem. Soc.* **1957**, *104* (3), 182.
- (103) Hu, X.; Tian, X.; Lin, Y.-W.; Wang, Z. J. R. a. Nickel foam and stainless steel mesh as electrocatalysts for hydrogen evolution reaction, oxygen evolution reaction and overall water splitting in alkaline media. *RSC Adv.* **2019**, *9* (54), 31563–31571. Lin, Y.; Sun, K.; Chen, X.; Chen, C.; Pan, Y.; Li, X.; Zhang, J. High-precision regulation synthesis of Fe-doped Co2P nanorod bundles as efficient electrocatalysts for hydrogen evolution in all-pH range and seawater. *J. Energy Chem.* **2021**, *55*, 92–101.
- (104) Mahmood, N.; Yao, Y.; Zhang, J. W.; Pan, L.; Zhang, X.; Zou, J. J. Electrocatalysts for hydrogen evolution in alkaline electrolytes: mechanisms, challenges, and prospective solutions. *Adv. Sci.* **2018**, *5* (2), 1700464.
- (105) Ali Shah, S.; Xu, L.; Sayyar, R.; Bian, T.; Liu, Z.; Yuan, A.; Shen, X.; Khan, I.; Ali Tahir, A.; Ullah, H. J. C. E. J. Growth of MoS2 nanosheets on M@ N-doped carbon particles (M= Co, Fe or CoFe Alloy) as an efficient electrocatalyst toward hydrogen evolution reaction. *Chem. Eng. J.* **2022**, *428*, 132126. Li, Y.; Li, H.; Li, Y.; Peng, S.; Hu, Y. Fe-B alloy coupled with Fe clusters as an efficient cocatalyst for photocatalytic hydrogen evolution. *Chem. Eng. J.* **2018**, *344*, 506–513.
- (106) Müller, C. I.; Rauscher, T.; Schmidt, A.; Schubert, T.; Weißgärber, T.; Kieback, B.; Röntzsch, L. Electrochemical investigations on amorphous Fe-base alloys for alkaline water electrolysis. *Int. J. Hydrogen Energy* **2014**, *39* (17), 8926–8937. Schäfer, H.; Chatenet, M. J. A. E. L. Steel: the resurrection of a forgotten water-splitting catalyst. *ACS Energy Lett.* **2018**, *3* (3), 574–591.
- (107) Ekspong, J.; Wågberg, T. J. M. Stainless steel as a bi-functional electrocatalyst—A top-down approach. *Materials* **2019**, *12* (13), 2128. Benavente Llorente, V.; Diaz, L. A.; Lacconi, G. I.; Abuin, G. C.;

- Franceschini, E. A. J. o. A. Compounds. Effect of duty cycle on NiMo alloys prepared by pulsed electrodeposition for hydrogen evolution reaction. *J. Alloys Compounds* **2022**, *897*, 163161. Nandanapalli, K. R.; Mudusu, D.; Karuppanan, R.; Hahn, Y.-B.; Lee, S. J. C. E. J. Predominantly enhanced catalytic activities of surface protected ZnO nanorods integrated stainless-steel mesh structures: A synergistic impact on oxygen evolution reaction process. *Chem. Eng. J.* **2022**, *429*, 132360.
- (108) Kim, M.; Ha, J.; Shin, N.; Kim, Y.-T.; Choi, J. J. E. A. Self-activated anodic nanoporous stainless steel electrocatalysts with high durability for the hydrogen evolution reaction. *Electrochim. Acta* **2020**, *364*, 137315.
- (109) Liu, X.; You, B.; Sun, Y. J. A. S. C. Engineering. Facile surface modification of ubiquitous stainless steel led to competent electrocatalysts for overall water splitting. *ACS Sustainable Chemistry* **2017**, *5* (6), 4778–4784. Zayat, B.; Mitra, D.; Narayanan, S. R. Inexpensive and efficient alkaline water electrolyzer with robust steel-based electrodes. *J. Electrochem. Soc.* **2020**, *167* (11), 114513. Gao, Y.; Xiong, T.; Li, Y.; Huang, Y.; Li, Y.; Balogun, M.-S. J. T. A simple and scalable approach to remarkably boost the overall water splitting activity of stainless steel electrocatalysts. *ACS Omega* **2019**, *4* (14), 16130–16138.
- (110) Yang, C.; Zhao, R.; Xiang, H.; Wu, J.; Zhong, W.; Li, W.; Zhang, Q.; Yang, N.; Li, X. Ni-activated transition metal carbides for efficient hydrogen evolution in acidic and alkaline solutions. *Adv. Energy Mater.* **2020**, *10* (37), 2002260. Jun, H.; Kim, S.; Lee, J. Development strategies in transition metal carbide for hydrogen evolution reaction: A review. *Korean Journal of Chemical Engineering* **2020**, *37* (8), 1317–1330. Peng, O.; Hu, Q.; Zhou, X.; Zhang, R.; Du, Y.; Li, M.; Ma, L.; Xi, S.; Fu, W.; Xu, Z.-X.; et al. Swinging hydrogen evolution to nitrate reduction activity in molybdenum carbide by ruthenium doping. *ACS Catal.* **2022**, *12* (24), 15045–15055.
- (111) Chen, P.; Ye, J.; Wang, H.; Ouyang, L.; Zhu, M. Recent progress of transition metal carbides/nitrides for electrocatalytic water splitting. *J. Alloys Compd.* **2021**, *883*, 160833. He, C.; Tao, J. Transition metal carbides coupled with nitrogen-doped carbon as efficient and stable Bi-functional catalysts for oxygen reduction reaction and hydrogen evolution reaction. *Int. J. Hydrogen Energy* **2022**, *47* (27), 13240–13250.
- (112) Zhang, X.; Zhu, Z.; Liang, X.; Ma, F.-X.; Zhang, J.; Tan, Y.; Pan, Z.; Bo, Y.; Wu, C.-M. L. Encapsulating dual-phased Mo₂C-WC nanocrystals into ultrathin carbon nanosheet assemblies for efficient electrocatalytic hydrogen evolution. *Chem. Eng. J.* **2021**, *408*, 127270. Yan, P.; Wu, Y.; Wei, X.; Zhu, X.; Su, W. Preparation of robust hydrogen evolution reaction electrocatalyst WC/C by molten salt. *Nanomaterials* **2020**, *10* (9), 1621. Hu, Z.; Chen, J.; Pan, P.; Liu, C.; Zeng, J.; Ou, Y.; Qi, X.; Liang, T. Porous N-doped Mo₂C@C nanoparticles for high-performance hydrogen evolution reaction. *Int. J. Hydrogen Energy* **2022**, *47* (7), 4641–4652.
- (113) Lv, Z.; Liu, D.; Tian, W.; Dang, J. Designed synthesis of WC-based nanocomposites as low-cost, efficient and stable electrocatalysts for the hydrogen evolution reaction. *CrystEngComm* **2020**, *22* (27), 4580–4590.
- (114) Wang, F.; Wu, Y.; Dong, B.; Lv, K.; Shi, Y.; Ke, N.; Hao, L.; Yin, L.; Bai, Y.; Xu, X.; et al. Robust Porous WC-Based Self-Supported Ceramic Electrodes for High Current Density Hydrogen Evolution Reaction. *Adv. Sci.* **2022**, *9*, 2106029. Huang, J.; Jian, C.; Cai, Q.; Hong, W.; Liu, W. A large scale self-supported WP-W₂C nanoporous network for efficient hydrogen evolution reaction in alkaline media. *J. Mater. Chem. A* **2022**, *10*, 10990.
- (115) Morishita, M.; Nozaki, A.; Yamamoto, H.; Fukumuro, N.; Mori, M.; Araki, K.; Sakamoto, F.; Nakamura, A.; Yanagita, H. Catalytic activity of Co-nanocrystal-doped tungsten carbide arising from an internal magnetic field. *RSC Adv.* **2021**, *11* (23), 14063–14070. Tian, D.; Denny, S. R.; Li, K.; Wang, H.; Kattel, S.; Chen, J. G. Density functional theory studies of transition metal carbides and nitrides as electrocatalysts. *Chem. Soc. Rev.* **2021**, *50*, 12338.
- (116) Ma, L.; Ting, L. R. L.; Molinari, V.; Giordano, C.; Yeo, B. S. Efficient hydrogen evolution reaction catalyzed by molybdenum carbide and molybdenum nitride nanocatalysts synthesized via the urea glass route. *Journal of Materials Chemistry A* **2015**, *3* (16), 8361–8368.
- (117) Liu, W.; Wang, X.; Wang, F.; Du, K.; Zhang, Z.; Guo, Y.; Yin, H.; Wang, D. A durable and pH-universal self-standing MoC-Mo₂C heterojunction electrode for efficient hydrogen evolution reaction. *Nat. Commun.* **2021**, *12* (1), 1–10.
- (118) Ji, X.; Wang, K.; Zhang, Y.; Sun, H.; Zhang, Y.; Ma, T.; Ma, Z.; Hu, P.; Qiu, Y. MoC based Mott-Schottky electrocatalyst for boosting the hydrogen evolution reaction performance. *Sustainable Energy & Fuels* **2020**, *4* (1), 407–416.
- (119) Hu, W.; Zheng, M.; Xu, B.; Wei, Y.; Zhu, W.; Li, Q.; Pang, H. Design of hollow carbon-based materials derived from metal-organic frameworks for electrocatalysis and electrochemical energy storage. *Journal of Materials Chemistry A* **2021**, *9* (7), 3880–3917.
- (120) Chen, Y.; Li, T.; Zhao, Q.; Liu, D.; Li, C. M. The in situ preparation of iron phosphide using ionic liquids as iron and phosphorus sources for efficient hydrogen evolution reactions. *RSC Adv.* **2020**, *10* (55), 33026–33032. Zhou, Q.; Wang, D. 3D nanoporous NiCoP as a highly efficient electrocatalyst for the hydrogen evolution reaction in alkaline electrolyte. *New J. Chem.* **2022**, *46* (16), 7490–7496.
- (121) Kumari, A.; Kaushal, S.; Singh, P. P. Bimetallic metal organic frameworks heterogeneous catalysts: Design, construction, and applications. *Materials Today Energy* **2021**, *20*, 100667. Sirisomboonchai, S.; Kitiphatpiboon, N.; Chen, M.; Li, S.; Li, X.; Kongparakul, S.; Samart, C.; Zhang, L.; Abudula, A.; Guan, G. Multi-Hierarchical Porous Mn-Doped CoP Catalyst on Nickel Phosphide Foam for Hydrogen Evolution Reaction. *ACS Appl. Energy Mater.* **2022**, *5* (1), 149–158. Park, Y.; Kang, H.; Hong, Y.-k.; Cho, G.; Choi, M.; Cho, J.; Ha, D.-H. Influence of the phosphorus source on iron phosphide nanoparticle synthesis for hydrogen evolution reaction catalysis. *Int. J. Hydrogen Energy* **2020**, *45* (57), 32780–32788.
- (122) Zhang, C.; Li, D.; Xu, Y. Mn-doped NiP: Facile synthesis and enhanced electrocatalytic activity for hydrogen evolution. *J. Mater. Res.* **2022**, *37* (3), 807–817.
- (123) Wang, Y.; Wang, Y.; Bai, J.; Lau, W.-M. Trace Amount of NiP₂ Cooperative CoMoP Nanosheets Inducing Efficient Hydrogen Evolution. *ACS omega* **2021**, *6* (48), 33057–33066.
- (124) Ge, L.; Yuan, H.; Min, Y.; Li, L.; Chen, S.; Xu, L.; Goddard III, W. A. Predicted optimal bifunctional electrocatalysts for the hydrogen evolution reaction and the oxygen evolution reaction using chalcogenide heterostructures based on machine learning analysis of in silico quantum mechanics based high throughput screening. *J. Phys. Chem. Lett.* **2020**, *11* (3), 869–876.
- (125) Tseng, C.-A.; Lee, C.-P. Transition Metal Chalcogenides for the Electrocatalysis of Water. In *Advanced Functional Materials*; IntechOpen: London, 2020. Iffelsberger, C.; Ng, S.; Pumera, M. Catalyst coating of 3D printed structures via electrochemical deposition: Case of the transition metal chalcogenide MoS_x for hydrogen evolution reaction. *Appl. Mater. Today* **2020**, *20*, 100654. Moschkowitsch, W.; Lori, O.; Elbaz, L. Recent Progress and Viability of PGM-Free Catalysts for Hydrogen Evolution Reaction and Hydrogen Oxidation Reaction. *ACS Catal.* **2022**, *12* (2), 1082–1089.
- (126) Ali, T.; Qiao, W.; Zhang, D.; Liu, W.; Sajjad, S.; Yan, C.; Su, R. Surface sulfur vacancy engineering of metal sulfides promoted desorption of hydrogen atoms for enhanced electrocatalytic hydrogen evolution. *J. Phys. Chem. C* **2021**, *125* (23), 12707–12712. Duraisamy, S.; Ganguly, A.; Sharma, P. K.; Benson, J.; Davis, J.; Papakonstantinou, P. One-step hydrothermal synthesis of phase-engineered MoS₂/MoO₃ electrocatalysts for hydrogen evolution reaction. *ACS Appl. Nano Mater.* **2021**, *4* (3), 2642–2656.
- (127) Mei, X.; Li, C.; Lam, F. L.-Y.; Hu, X. Nanosheet-like ternary metal sulfide as a pH-universal catalyst for the hydrogen evolution reaction. *ACS Appl. Energy Mater.* **2020**, *3* (7), 6172–6179. Aslan, E.; Yanalak, G.; Hatay Patir, I. Enhanced Hydrogen Evolution Reaction Catalysis at Template-Free Liquid/Liquid Interfaces by In Situ Electrodeposited Amorphous Molybdenum Sulfide on Carbon Nanotubes. *ACS Appl. Energy Mater.* **2021**, *4* (8), 8330–8339.

- (128) Wang, S.; Huang, B.; Dai, Y.; Wei, W. Origin of the Enhanced Hydrogen Evolution Reaction Activity of Grain Boundaries in MoS₂ Monolayers. *J. Phys. Chem. C* **2022**, *126* (14), 6215–6222. Zhou, W.; Dong, L.; Tan, L.; Tang, Q. First-principles study of sulfur vacancy concentration effect on the electronic structures and hydrogen evolution reaction of MoS₂. *Nanotechnology* **2021**, *32* (14), 145718.
- (129) He, M.; Kong, F.; Yin, G.; Lv, Z.; Sun, X.; Shi, H.; Gao, B. Enhanced hydrogen evolution reaction activity of hydrogen-annealed vertical MoS₂ nanosheets. *RSC Adv.* **2018**, *8* (26), 14369–14376.
- (130) Zhu, J.; Tu, Y.; Cai, L.; Ma, H.; Chai, Y.; Zhang, L.; Zhang, W. Defect-Assisted Anchoring of Pt Single Atoms on MoS₂ Nanosheets Produces High-Performance Catalyst for Industrial Hydrogen Evolution Reaction. *Small* **2022**, *18* (4), 2104824. Zheng, J.; Lu, L.; Lebedev, K.; Wu, S.; Zhao, P.; McPherson, I. J.; Wu, T.-S.; Kato, R.; Li, Y.; Ho, P.-L.; et al. Fe on molecular-layer MoS₂ as inorganic Fe-S₂-Mo motifs for light-driven nitrogen fixation to ammonia at elevated temperatures. *Chem. Catalysis* **2021**, *1* (1), 162–182.
- (131) Zheng, Z.; Yu, L.; Gao, M.; Chen, X.; Zhou, W.; Ma, C.; Wu, L.; Zhu, J.; Meng, X.; Hu, J.; et al. Boosting hydrogen evolution on MoS₂ via co-confining selenium in surface and cobalt in inner layer. *Nat. Commun.* **2020**, *11* (1), 1–10.
- (132) Kazemi Korayem, A.; Ghamami, S.; Bahrami, Z. Fractal properties and morphological investigation of nano-amiodarone using image processing. *Signal Image Video Process.* **2019**, *13* (2), 281–287. Guo, B.; Yu, K.; Li, H.; Qi, R.; Zhang, Y.; Song, H.; Tang, Z.; Zhu, Z.; Chen, M. Coral-shaped MoS₂ decorated with graphene quantum dots performing as a highly active electrocatalyst for hydrogen evolution reaction. *ACS Appl. Mater. Interfaces* **2017**, *9* (4), 3653–3660. Park, T.; Bae, C.; Lee, H.; Leem, M.; Kim, H.; Ahn, W.; Kim, J.; Lee, E.; Shin, H.; Kim, H. Non-equilibrium fractal growth of MoS₂ for electrocatalytic hydrogen evolution. *CrystEngComm* **2019**, *21* (3), 478–486. Kazemi Korayem, A.; Ghamami, S.; Bahrami, Z. Fractal properties and morphological investigation of Nano hydrochlorothiazide is used to treat hypertension. *BMC Pharmacol. Toxicol.* **2018**, *19*, 1–9.
- (133) Ge, Y.; Shi, Z.; Tan, C.; Chen, Y.; Cheng, H.; He, Q.; Zhang, H. Two-dimensional nanomaterials with unconventional phases. *Chem.* **2020**, *6* (6), 1237–1253. Ma, X.; Yang, J.; Xu, X.; Yang, H.; Peng, C. NiSe/Ni₃Se₂ on nickel foam as an ultra-high-rate HER electrocatalyst: common anion heterostructure with built-in electric field and efficient interfacial charge transfer. *RSC Adv.* **2021**, *11* (55), 34432–34439.
- (134) Deng, W.; Xie, W.; Li, D.; Gai, Y.; Chen, Z.; Yu, J.; Yang, R.; Bao, X.; Jiang, F. Controllable tuning of polymetallic Co-Ni-Ru-S-Se ultrathin nanosheets to boost electrocatalytic oxygen evolution. *NPG Asia Mater.* **2022**, *14* (1), 1–13.
- (135) Wang, K.; Lin, Z.; Tang, Y.; Tang, Z.; Tao, C.-L.; Qin, D.-D.; Tian, Y. Selenide/sulfide heterostructured NiCo₂Se₄/NiCoS₄ for oxygen evolution reaction, hydrogen evolution reaction, water splitting and Zn-air batteries. *Electrochim. Acta* **2021**, *368*, 137584. Pang, Y.; Zhu, S.; Cui, Z.; Liang, Y.; Li, Z.; Wu, S. Self-supported amorphous nanoporous nickel-cobalt phosphide catalyst for hydrogen evolution reaction. *Progress in Natural Science: Materials International* **2021**, *31* (2), 201–206.
- (136) Xiao, D.; Bao, D.-L.; Liang, X.; Wang, Y.; Shen, J.; Cheng, C.; Chu, P. K. Experimental and theoretical investigation of the control and balance of active sites on oxygen plasma-functionalized MoSe₂ nanosheets for efficient hydrogen evolution reaction. *Appl. Catal. B: Environmental* **2021**, *288*, 119983.
- (137) Chang, Y.; Chen, C.; Ho, C.; Cheng, C.; Chen, H.; Fu, T.; Huang, Y.; Ke, S.; Du, H.; Lee, K.; et al. Surface electron accumulation and enhanced hydrogen evolution reaction in MoSe₂ basal planes. *Nano Energy* **2021**, *84*, 105922.
- (138) Yang, X.; Liu, W.; Han, C.; Zhao, C.; Tang, H.; Liu, Q.; Xu, J. Mechanistic insights into charge carrier dynamics in MoSe₂/CdS heterojunctions for boosted photocatalytic hydrogen evolution. *Materials Today Physics* **2020**, *15*, 100261. Ruqia, B.; Kabiraz, M. K.; Hong, J. W.; Choi, S.-I. Catalyst activation: Surface doping effects of group VI transition metal dichalcogenides towards hydrogen evolution reaction in acidic media. *J. Energy Chem.* **2022**, *72*, 217.
- (139) Wu, P.; Sun, G.; Chen, Y.; Xu, W.; Zheng, H.; Xu, J.; Wang, L.; Peng, D.-L. MoSe₂-Ni₃Se₄ hybrid nanoelectrocatalysts and their enhanced electrocatalytic activity for hydrogen evolution reaction. *Nanoscale Res. Lett.* **2020**, *15* (1), 1–10.
- (140) Hu, W.; Shi, Q.; Chen, Z.; Yin, H.; Zhong, H.; Wang, P. Co₂N/Co₂Mo₃O₈ heterostructure as a highly active electrocatalyst for an alkaline hydrogen evolution reaction. *ACS Appl. Mater. Interfaces* **2021**, *13* (7), 8337–8343. Dan, Z.; Liang, W.; Gong, X.; Lin, X.; Zhang, W.; Le, Z.; Xie, F.; Chen, J.; Yang, M.; Wang, N.; et al. Substitutional Doping Engineering toward W₂N Nanorod for Hydrogen Evolution Reaction at High Current Density. *ACS Mater. Lett.* **2022**, *4* (7), 1374–1380.
- (141) Tong, R.; Xu, M.; Huang, H.; Zhang, C.; Ma, Y.; Wang, X.; Hu, X.; Qu, Y.; Wang, S.; Pan, H. Co₂N_{0.67}/MoO₂ Heterostructure as High-Efficiency Electrocatalysts for the Hydrogen Evolution Reaction. *ACS Appl. Energy Mater.* **2022**, *5* (1), 440–448. Xing, Z.; Li, Q.; Wang, D.; Yang, X.; Sun, X. Self-supported nickel nitride as an efficient high-performance three-dimensional cathode for the alkaline hydrogen evolution reaction. *Electrochim. Acta* **2016**, *191*, 841–845.
- (142) Zhou, W.; Huang, S.; Sun, C. Ni₃Mo₃N coupled with nitrogen-rich carbon microspheres as an efficient hydrogen evolution reaction catalyst and electrochemical sensor for H₂O₂ detection. *Int. J. Hydrogen Energy* **2022**, *47* (33), 14906–14915.
- (143) Park, S. H.; Kang, S. H.; Youn, D. H. Direct One-Step Growth of Bimetallic Ni₂Mo₃N on Ni Foam as an Efficient Oxygen Evolution Electrocatalyst. *Materials* **2021**, *14* (16), 4768.
- (144) Wang, C.; Lv, X.; Zhou, P.; Liang, X.; Wang, Z.; Liu, Y.; Wang, P.; Zheng, Z.; Dai, Y.; Li, Y. Molybdenum nitride electrocatalysts for hydrogen evolution more efficient than platinum/carbon: Mo₂N/CeO₂@ nickel foam. *ACS Appl. Mater. Interfaces* **2020**, *12* (26), 29153–29161.
- (145) Balaji, D.; Madhavan, J.; AlSalhi, M. S.; Aljaafreh, M. J.; Prasad, S.; Show, P. L. Carbon supported Ni₃N/Ni heterostructure for hydrogen evolution reaction in both acid and alkaline media. *Int. J. Hydrogen Energy* **2021**, *46* (60), 30739–30749.
- (146) Zhang, J.; Zhang, L.; Du, L.; Xin, H. L.; Goodenough, J. B.; Cui, Z. Composition-Tunable Antiperovskite Cu_xIn_{1-x}Ni₃ as Superior Electrocatalysts for the Hydrogen Evolution Reaction. *Angew. Chem., Int. Ed.* **2020**, *59* (40), 17488–17493.
- (147) Dastafkan, K.; Shen, X.; Hocking, R. K.; Meyer, Q.; Zhao, C. Monometallic interphasic synergy via nano-hetero-interfacing for hydrogen evolution in alkaline electrolytes. *Nat. Commun.* **2023**, *14* (1), 547.
- (148) Wang, H.-F.; Chen, L.; Pang, H.; Kaskel, S.; Xu, Q. MOF-derived electrocatalysts for oxygen reduction, oxygen evolution and hydrogen evolution reactions. *Chem. Soc. Rev.* **2020**, *49* (5), 1414–1448. Sahu, N.; Das, J. K.; Behera, J. NiSe₂ Nanoparticles Encapsulated in N-Doped Carbon Matrix Derived from a One-Dimensional Ni-MOF: An Efficient and Sustained Electrocatalyst for Hydrogen Evolution Reaction. *Inorg. Chem.* **2022**, *61* (6), 2835–2845. Aleksandrak, M.; Sielicki, K.; Mijowska, E. Enhancement of photocatalytic hydrogen evolution with catalysts based on carbonized MOF-5 and gC₃N₄. *RSC Adv.* **2020**, *10* (7), 4032–4039.
- (149) Wang, X.; Maeda, K.; Thomas, A.; Takanabe, K.; Xin, G.; Carlsson, J. M.; Domen, K.; Antonietti, M. A metal-free polymeric photocatalyst for hydrogen production from water under visible light. *Nature materials* **2009**, *8* (1), 76–80. Sprick, R. S.; Bonillo, B.; Clowes, R.; Guiglion, P.; Brownbill, N. J.; Slater, B. J.; Blanc, F.; Zwijnenburg, M. A.; Adams, D. J.; Cooper, A. I. Visible-light-driven hydrogen evolution using planarized conjugated polymer photocatalysts. *Angew. Chem., Int. Ed.* **2016**, *55* (5), 1792–1796. Rahman, M. Z.; Davey, K.; Qiao, S.-Z. Carbon, nitrogen and phosphorus containing metal-free photocatalysts for hydrogen production: progress and challenges. *J. Mater. Chem. A* **2018**, *6* (4), 1305–1322. Gopi, S.; Panda, A.; Ramu, A.; Theerthagiri, J.; Kim, H.; Yun, K. J. Bifunctional electrocatalysts for water splitting from a bimetallic (V doped-NixFey) Metal-Organic framework MOF@ Graphene oxide composite. *Int. J. Hydrogen Energy* **2022**, *47*, 42122. Liu, Y.; Cheng, H.; Cheng, M.; Liu, Z.; Huang, D.; Zhang, G.; Shao, B.; Liang, Q.; Luo, S.; Wu, T. J. C. E. J.; et al. The application of Zeolitic

imidazolate frameworks (ZIFs) and their derivatives based materials for photocatalytic hydrogen evolution and pollutants treatment. *Chem. Eng. J.* **2021**, *417*, 127914.

(150) Zhu, B.; Qu, C.; Gao, S.; Liang, Z.; Zhang, H.; Zou, R. J. C. Ultralow Loading Ruthenium Nanoparticles on Nitrogen-Doped Graphene Aerogel for Trifunctional Electrocatalysis. *ChemCatChem*. **2018**, *10* (5), 1113–1121. Zhu, B.; Wen, D.; Liang, Z.; Zou, R. J. C. R. Conductive metal-organic frameworks for electrochemical energy conversion and storage. *Coord. Chem. Rev.* **2021**, *446*, 214119.

(151) Gao, H.; Shen, H.; Wu, H.; Jing, H.; Sun, Y.; Liu, B.; Chen, Z.; Song, J.; Lu, L.; Wu, Z. J. E.; et al. Review of Pristine Metal-Organic Frameworks for Supercapacitors: Recent Progress and Perspectives. *Energy Fuels* **2021**, *35* (16), 12884–12901. Qiu, T.; Gao, S.; Liang, Z.; Wang, D. G.; Tabassum, H.; Zhong, R.; Zou, R. J. A. C. I. E. Pristine Hollow Metal-Organic Frameworks: Design, Synthesis and Application. *Angew. Chem., Int. Ed.* **2021**, *60*, 17314.

(152) Sonowal, K.; Saikia, L. Metal-organic frameworks and their composites for fuel and chemical production via CO₂ conversion and water splitting. *RSC Adv.* **2022**, *12* (19), 11686–11707. Li, P.; Zheng, D.; Gao, M.; Zuo, X.; Sun, L.; Zhou, Q.; Lin, J. Bimetallic MOF-Templated Fabrication of Porous Zn, N Co-doped Mo₂C for an Efficient Hydrogen Evolution Reaction. *ACS Appl. Energy Mater.* **2021**, *4* (9), 8875–8882. Zheng, H.-b.; Chen, H.-h.; Wang, Y.-l.; Gao, P.-z.; Liu, X.-p.; Rebrov, E. V. Fabrication of magnetic superstructure NiFe₂O₄@ MOF-74 and its derivative for electrocatalytic hydrogen evolution with AC magnetic field. *ACS Appl. Mater. Interfaces* **2020**, *12* (41), 45987–45996.

(153) Ao, K.; Wei, Q.; Daoud, W. A. MOF-derived sulfide-based electrocatalyst and scaffold for boosted hydrogen production. *ACS Appl. Mater. Interfaces* **2020**, *12* (30), 33595–33602. Qi, W.; Wang, C.; Yu, J.; Adimi, S.; Thomas, T.; Guo, H.; Liu, S.; Yang, M. MOF-Derived Porous Ternary Nickel Iron Nitride Nanocube as a Functional Catalyst toward Water Splitting Hydrogen Evolution for Solar to Chemical Energy Conversion. *ACS Appl. Energy Mater.* **2022**, *5*, 6155.

(154) Kazemi, A.; Moghadaskhou, F.; Pordsari, M. A.; Manteghi, F.; Tadjarodi, A.; Ghaemi, A. Enhanced CO₂ capture potential of UiO-66-NH₂ synthesized by sonochemical method: experimental findings and performance evaluation. *Sci. Rep.* **2023**, *13* (1), 19891. Ramezanalizadeh, H.; Manteghi, F. Mixed cobalt/nickel metal-organic framework, an efficient catalyst for one-pot synthesis of substituted imidazoles. *Monatshefte für Chemie-Chemical Monthly* **2017**, *148*, 347–355. Ramezanalizadeh, H.; Manteghi, F. Synthesis of a novel MOF/CuWO₄ heterostructure for efficient photocatalytic degradation and removal of water pollutants. *Journal of Cleaner Production* **2018**, *172*, 2655–2666. Abhari, P. S.; Manteghi, F.; Tehrani, Z. Adsorption of lead ions by a green AC/HKUST-1 nanocomposite. *Nanomaterials* **2020**, *10* (9), 1647.

(155) Li, Y.-W.; Wu, Q.; Ma, R.-C.; Sun, X.-Q.; Li, D.-D.; Du, H.-M.; Ma, H.-Y.; Li, D.-C.; Wang, S.-N.; Dou, J.-M. A Co-MOF-derived Co₉S₈@ NS-C electrocatalyst for efficient hydrogen evolution reaction. *RSC Adv.* **2021**, *11* (11), 5947–5957. Sun, Y.; Xue, Z.; Liu, Q.; Jia, Y.; Li, Y.; Liu, K.; Lin, Y.; Liu, M.; Li, G.; Su, C.-Y. Modulating electronic structure of metal-organic frameworks by introducing atomically dispersed Ru for efficient hydrogen evolution. *Nat. Commun.* **2021**, *12* (1), 1369.

(156) Yan, L.; Cao, L.; Dai, P.; Gu, X.; Liu, D.; Li, L.; Wang, Y.; Zhao, X. J. A. F. M. Metal-organic frameworks derived nanotube of nickel-cobalt bimetal phosphides as highly efficient electrocatalysts for overall water splitting. *Adv. Funct. Mater.* **2017**, *27* (40), 1703455.

(157) Hao, X.; Jin, Z.; Yang, H.; Lu, G.; Bi, Y. J. A. C. B. E. Peculiar synergetic effect of MoS₂ quantum dots and graphene on Metal-Organic Frameworks for photocatalytic hydrogen evolution. *Appl. Catal. B.: Environ.* **2017**, *210*, 45–56.

(158) Zhen, W.; Ma, J.; Lu, G. Small-sized Ni (1 1 1) particles in metal-organic frameworks with low over-potential for visible photocatalytic hydrogen generation. *Appl. Catal. B: Environmental* **2016**, *190*, 12–25.

(159) Li, Y.; Ai, C.; Deng, S.; Wang, Y.; Tong, X.; Wang, X.; Xia, X.; Tu, J. Nitrogen doped vertical graphene as metal-free electrocatalyst for hydrogen evolution reaction. *Mater. Res. Bull.* **2021**, *134*, 111094.